glucose- and carbachol-stimulated insulin secretion was restored (Fig. 4B and C), indicating reduced insulin secretion in islets from mutant mice to be a direct consequence of absence of normal WFS1 function. Interestingly, glucose- and carbachol-stimulated insulin secretion from wild-type islets increased by 41 and 53%, respectively, with overexpression of the WFS1 protein, suggesting involvement of the WFS1 protein in stimulus–secretion coupling for insulin exocytosis (Fig. 4B and C).

To gain insight into the mechanisms of impaired insulin secretion in islets from mutant mice, intracellular calcium dynamics were then studied in single β-cells challenged with glucose. The glucose-stimulated rise in the cytosolic Ca^{2+} response was reduced by 36% in WFS1-deficient β-cells when compared with that in wild-type β-cells (Fig. 4D and E).

Progressive β-cell loss in mutant mice

We then focused on aspects of insulin production, deterioration of which could be a cause of impaired glucose homeostasis in mice with disruption of the *wfs1* gene. There were no differences in pancreatic weight between wild-type and mutant mice (data not shown). Whole-pancreas insulin content was already decreased at 2 weeks, the earliest age studied, and dropped further with age (Fig. 5A). Immunohistochemical studies (Fig. 5B–E) showed the number of insulin-positive cells to be reduced at 36 weeks in the mutant mouse pancreas (Fig. 5E). Morphometric analysis demonstrated a marked reduction in the insulin-positive area per pancreatic area in mutant mice when compared with wild-type mice (Fig. 5H), indicating the decrease in insulin content to be due to loss of islet β-cells. These features were more prominent in the mutant mouse pancreas on the [(129Sv × B6) × B6]F2 background, which was associated with overt diabetes (Fig. 5F and G). In contrast to the β-cell changes, glucagon-positive cells were increased and scattered throughout WFS1-deficient islets (Fig. 5E and G). Indeed, the pancreatic glucagon content in mutant mice at 36 weeks of age on the B6 background was 2.4-fold higher than that in wild-type mice [12.3 ± 1.8 ng/mg ($n = 4$) versus 5.2 ± 0.7 ($n = 4$), $P = 0.0296$].

Increased susceptibility of WFS1-deficient islets to apoptosis

To study whether the observed β-cell loss was due to increased apoptosis, we conducted an extensive search for apoptotic β-cells in pancreatic sections. However, TUNEL or activated-caspase 3-positive cells were sparse within islets in pancreatic sections from both mutant and wild-type animals (data not shown). Therefore, we turned to *in vitro* studies, and examined whether WFS1-deficient islet cells are more susceptible to apoptotic insults. For this purpose, apoptotic DNA fragmentation was studied in isolated islets by the ligation-mediated PCR (LM-PCR) method. When islets were cultured for 3 days in RPMI media with 5 or 25 mM glucose, ladder formation was increased at 25 mM glucose in both wild-type and mutant islets when compared with that at 5 mM glucose, indicating that apoptotic cell death may have been induced by glucose toxicity (Fig. 6A). Importantly, at 25 mM glucose, islets from mutant mice showed more DNA fragment formation than wild-type islets (1.7 ± 0.3-fold, $n = 5$), while no significant differences were observed at 5 mM glucose. Since recent studies have suggested so-called ER-stress to be an important mediator of apoptosis in β-cells (14,15), DNA fragmentation was studied after treatment with two different ER-stress inducers (18), tunicamycin (2 μg/ml) and thapsigargin (2 μM). DNA fragmentation at 5 mM glucose was significantly increased, by 2.2 ± 0.4-fold and 2.4 ± 0.4-fold after tunicamycin (Fig. 6B) and thapsigargin (Fig. 6C) treatments, respectively, in WFS1-deficient islets when compared with wild-type islets. In contrast, there were no differences in DNA fragmentation after combined tumor necrosis factor-α and interferon-γ treatment (Fig. 6D), which triggers apoptosis through a signaling pathway different from that originating in the ER.

DISCUSSION

We generated mice with a disrupted *wfs1* gene. Although the diabetic phenotype was milder than that seen clinically in Wolfram syndrome (1), the progressive β-cell loss and impaired glucose homeostasis observed in these mice are essentially consistent with findings in patients (1,17). Thus, the mutant mice are indeed a model of Wolfram syndrome. The underlying anatomic condition of this syndrome has not been studied in great detail in humans, and the cellular basis for the diabetic phenotype and associated neuro-psychiatric disorders remains obscure. Creation of an animal model that reflects aspects of the disease is thus an important first step in understanding Wolfram syndrome.

The present data demonstrate that the pathophysiological basis of diabetes in Wolfram syndrome is insufficient insulin secretion due to progressive β-cell loss and impaired stimulus–secretion coupling in β-cells. Progressive β-cell loss has been expected from clinical observations of progressive deterioration of insulin-requiring states in affected patients as well as their postmortem findings, i.e. selective β-cell loss with an increase in α-cells and preservation of δ-cells (17). In contrast, impaired stimulus–secretion coupling in the β-cell, a quite unexpected result, was demonstrated for the first time in this study. In addition, we also showed for the first time that WFS1 protein is expressed selectively in β-cells, but very little in α, δ and F-cells, within the endocrine pancreas, suggesting that β-cell loss is a direct consequence of WFS1 deficiency.

The severity of the diabetic phenotype due to *wfs1* gene disruption was dependent on the mouse genetic background: >60% of mice on the [(129Sv × B6) × B6]F2 background developed overt diabetes, while mutant mice on the B6 background had impaired glucose tolerance but not overt diabetes. Modifying effects of genetic background on glucose homeostasis have been reported previously in a number of mutant mice. An earlier pioneering study established that the B6 background confers more diabetes resistance to db/db and ob/ob mice (19). A diabetes-resistant phenotype has also been reported in insulin receptor substrate (IRS)-2 knockout mice on the B6 background (20), while anti-sense glucokinase-mRNA expressing mice (21) and mice double heterozygous for deletion of the insulin receptor and IRS-1 (22), on the same B6 background, were reportedly diabetes prone. Therefore, the

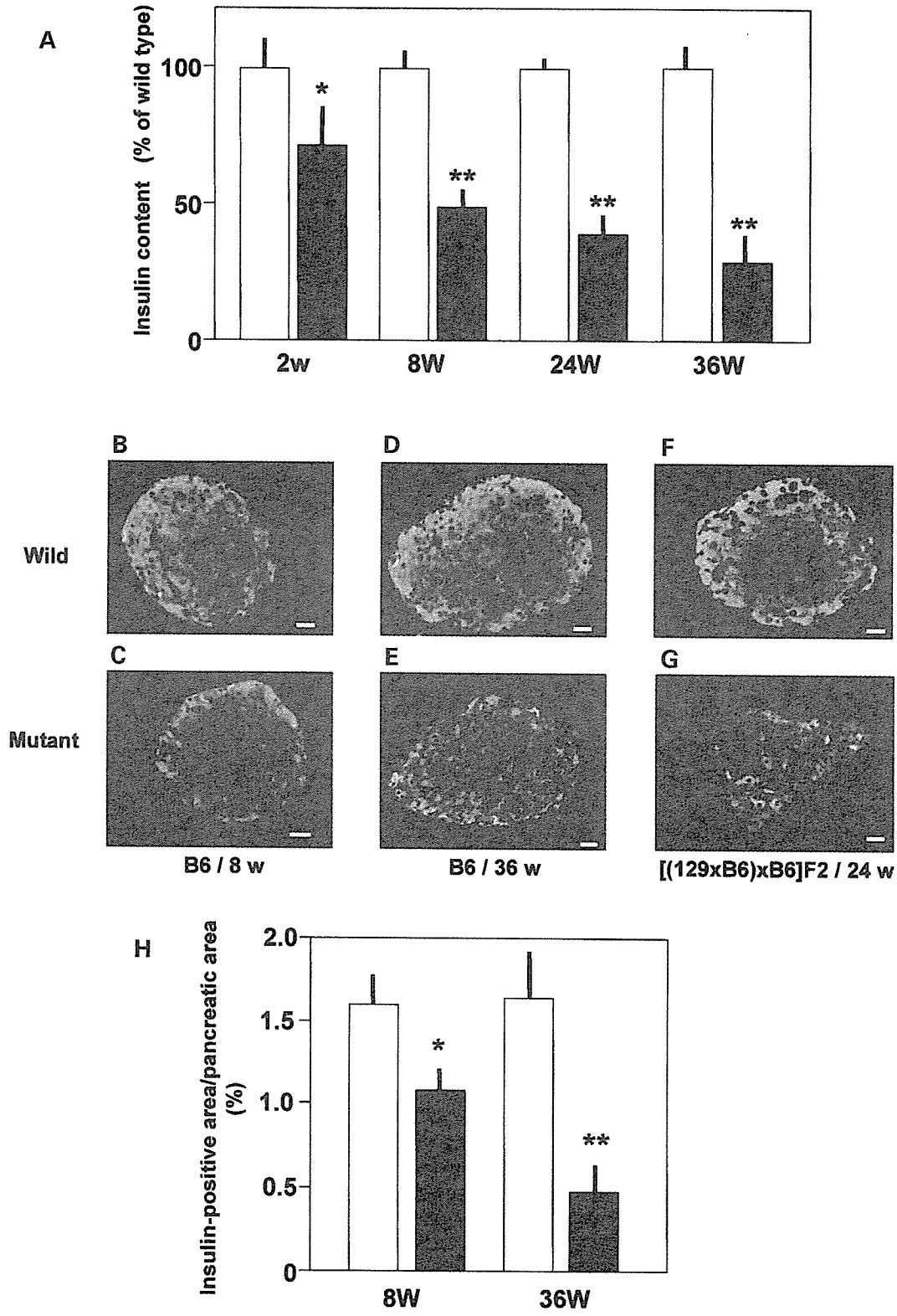

Figure 5. Progressive β-cell loss in mutant mice. (**A**) Insulin content extracted from whole pancreata of wild-type and mutant mice. Data represent percent of insulin content in wild-type littermates. Absolute insulin content in wild-type pancreata were 1367 ± 103 ng/mg pancreas at 2 weeks, 268 ± 18 (8 weeks), 329 ± 25 (24 weeks) and 372 ± 33 (36 weeks), $n = 4–7$. White bars, wild-type pancreata; black bars, WFS1-deficient pancreata. (**B–G**) Insulin (green) and glucagon (red) are stained in pancreatic sections from 8-week-old wild-type (B), mutant (C), 36-week-old wild-type (D) and mutant mice (E) on the B6 background, and 24-week-old wild-type (F) and mutant (G) mice on the [(129Sv × B6) × B6]F2 background. Bars = 10 μm. (**H**) Ratios of total insulin-positive area per whole pancreatic area in pancreas from wild-type and mutant mice on the B6 background. $n = 4$ animals for each group. $^{*}P < 0.05$, $^{**}P < 0.01$.

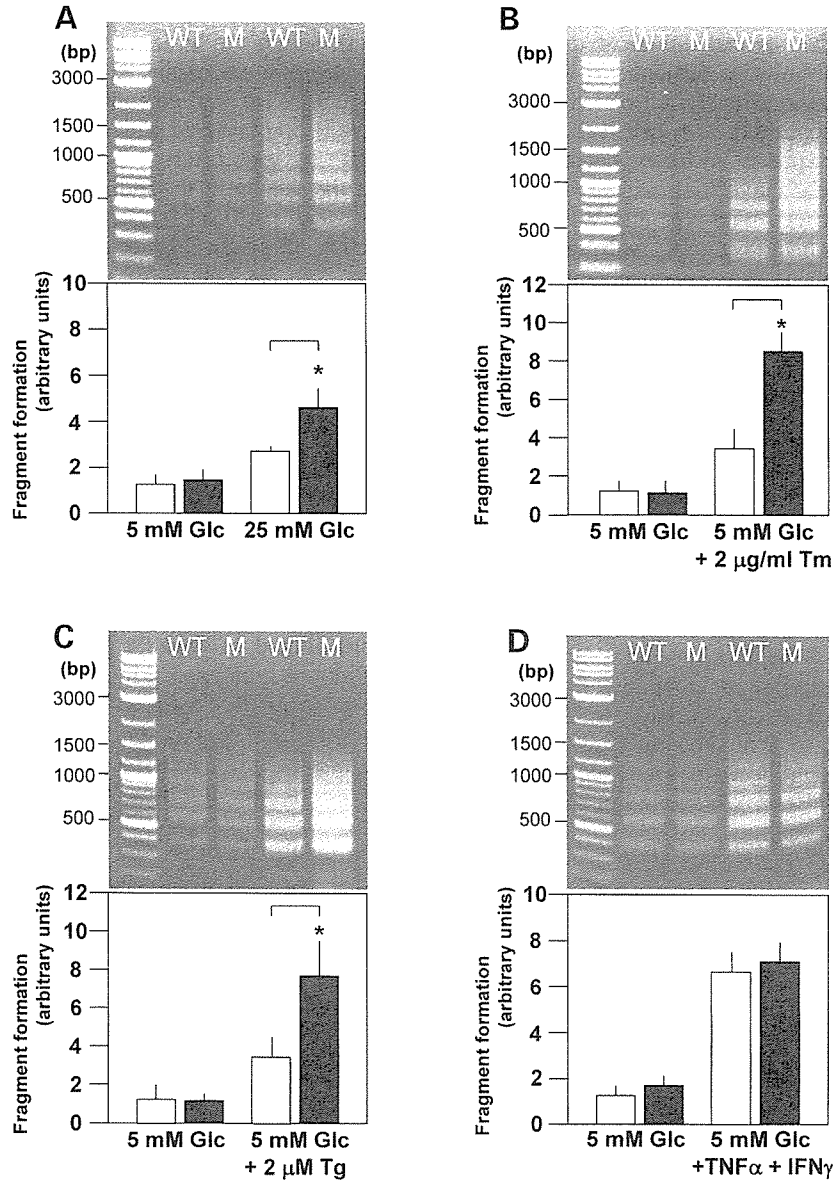

Figure 6. Increased apoptosis susceptibility in islets from mutant mice. (**A**) Islets from wild-type and mutant mice were cultured for 3 days in 5 and 25 mM glucose concentrations and DNA fragmentation was assessed by the LM-PCR method. (**B–D**) Islets from wild-type and mutant mice were treated with tunicamycin (Tm; 2 μg/ml) (B), thapsigargin (Tg; 2 μM) (C) for 24 h or with the combination of tumor necrosis factor-α (TNFα; 500 units/ml) and interferon-γ (IFNγ; 100 units/ml) (D) for 48 h and DNA fragmentation was assessed by the LM-PCR method; $n = 4–6$ experiments. $^*P < 0.05$.

contribution of genetic background is apparently complex. In any case, progressive β-cell loss was observed in mutant mice in both [(129Sv × B6) × B6]F2 and B6 strains, independent of the mouse genetic background. It is not surprising that mutant mice on the B6 background did not develop overt diabetes. Overt diabetes was known to be induced when >90% of the pancreas was removed (23), while the insulin content of mutant mouse pancreas at 36 weeks was decreased by 73% on the B6 background in this study.

The present data provide an intriguing clue that may help to elucidate WFS1 protein function. WFS1-deficient islets exhibited impaired insulin secretion in response to glucose and carbachol, which was restored by re-expression of WFS1 protein. In addition, overexpression of WFS1 protein in wild-type islets resulted in an increase in glucose- and carbachol-induced insulin secretion. These data from islets with different WFS1 protein levels demonstrated this protein to be involved directly in the regulation of insulin secretion. Furthermore, impaired calcium responses to glucose suggested that WFS1 protein is involved in regulation of calcium homeostasis in the β-cell. This notion is supported by the recent report that expression of WFS1 protein in *Xenopus* oocytes confers a novel cation channel activity (24). The present data also provide insight into the mechanism of β-cell loss in mice with a mutant *wfs1* gene. Although we rarely detected apoptotic cells in pancreatic sections from mutant mice, apoptosis cannot be excluded as a possible mechanism of β-cell loss, since our failure could presumably be due to slow progression of apoptosis *in vivo*

and rapid clearance of cells undergoing apoptosis, as was suggested recently in another animal model of diabetes (25). Increased apoptosis susceptibility in response to high glucose and ER-stress inducers, demonstrated in isolated islets from mutant mice, is likely to contribute to β-cell loss. In contrast, the apoptosis induced by exposure to tumor necrosis factor-α and interferon-γ, in which the ER-stress response is not involved, did not differ between wild-type and WFS1-deficient islets. Although the mechanism whereby high concentrations of glucose induce apoptosis is not completely understood at present (26,27), increased insulin translation in *perk*$^{-/-}$ islets indicates the ER-stress response or the unfolded protein response to be operative in islets cultured with high concentrations of glucose (28). Therefore, it is possible that increased DNA fragmentation in WFS1-deficient islets at 25 mM glucose could also be attributable to increased susceptibility to ER-stress-induced apoptosis. However, it remains to be clarified how WFS1 deficiency renders β-cells more susceptible to apoptosis, especially to ER-stress-induced apoptosis.

Recent studies showing β-cell mass to be decreased in human type 2 diabetes, due to increased β-cell apoptosis (29), have attracted considerable attention to this potential pathogenic mechanism of type 2 diabetes development. Therefore, maintaining β-cell mass is an important strategy for preventing diabetes as well as halting disease progression. Since the WFS1 protein is likely to belong to a novel family, elucidating the WFS1 protein function could lead to establishment of new treatments not only for Wolfram syndrome but also for more common forms of diabetes mellitus.

MATERIALS AND METHODS

Targeted disruption of the *wfs1* gene

The *wfs1* gene was cloned from a 129Sv mouse genomic DNA library using its cDNA probe (3). A targeting vector was constructed by inserting a neomycin-resistance gene at the *Sma*I site in exon 2 of the *wfs1* gene. The diphtheria toxin A chain expressing unit was inserted downstream (Fig. 2A). The *wfs1* gene targeting vector was microinjected into 129Sv embryonic stem cells. Homologous recombination was successful in two independent embryonic stem cell lines (lines 133 and 190). Positive chimeric male mice were then crossed with female C57BL/6J (B6) mice to produce *wfs1* heterozygous mice. Initial analyses demonstrated essentially the same phenotypes between the two lines, and therefore we have analyzed line 133 mice. In order to analyze animals with as homogenous a genetic background as possible, male *wfs1* heterozygous mice were backcrossed with female B6 mice for five successive generations. We also analyzed *wfs1* homozygous mice on the [(129Sv × B6) × B6]F2 hybrid background. The mice were kept in standard, specific pathogen-free conditions under a constant dark/light cycle. All animal experiments were approved by the local ethical committee for animal research at the Tohoku University.

Physiological studies

Control animals were age-matched siblings. Blood glucose levels in the non-fasting state were measured at 9:00–10:00 a.m. using a GluTest blood glucose monitor (Sanwa Chemicals, Tokyo, Japan). Serum insulin levels were determined by radioimmunoassay using a rat insulin RIA kit (Linco Research, St Charles, MO, USA). For oral glucose tolerance tests, animals after a 6 h fast were administered with 20% glucose solution (2 mg/g body weight) by gastric tubes. Whole-blood samples were collected from the tail tip at the indicated time points. Insulin tolerance tests were performed after a 6 h fast by an intraperitonial injection of human regular insulin (0.75 units/kg body weight).

Immunohistochemistry and morphometry

For brain sections, animals were anesthetized by ethylethel, and 4% formalin was perfused from the left ventricle. For pancreatic sections, the animals were killed by cervical dislocation. Dissected pancreas pieces were fixed in 4% formalin. Formalin-fixed paraffin-embedded sections of pancreas were de-paraffinized and re-hydrated. For insulin and glucagon staining, the sections were then incubated with a guinea pig anti-insulin IgG (DAKO Japan, Kyoto, Japan) diluted 1 : 1000 and a mouse anti-glucagon IgG (Sigma-Aldrich Japan, Tokyo, Japan) diluted 1 : 2000 for 1 h at room temperature. The anti-insulin and -glucagon primary antibodies were followed by a 45 min incubation with a fluorescein isothiocyanate (FITC)-conjugated anti-guinea pig IgG and a Texas Red-conjugated anti-mouse IgG (Jackson ImmunoResearch, West Grove, PA, USA). The antibody raised against the 290 amino acid α-mWFS1-N was described previously (30). Pancreatic sections incubated with the anti-WFS1 antibody were then stained with an FITC-conjugated anti-rabbit IgG (Jackson ImmunoResearch). Immunohistochemical analyses were performed, sacrificing at least four different animals for each condition. For measurements of β-cell area, more than 10 pancreatic tissue sections per animal were randomly selected, stained with anti-insulin IgG and eosin. Pancreatic area and β-cell area were each estimated using the intensity thresholding function of the NIH Image software. Four animals were analyzed for each group.

Pancreatic insulin and glucagon content

Pancreases were suspended in cold acid ethanol and minced by scissors, and left at −20°C for 48 h, with sonication every 24 h. Insulin content in the acid ethanol supernatant was determined with a rat insulin RIA Kit (Linco Research). Glucagon content in the same extract was measured by a glucagon RIA kit (Linco Research).

Islet studies

Construction of a recombinant adenovirus expressing murine WFS1 protein. A recombinant adenovirus AdCAGmWFS1, bearing an *Eco*RI fragment of murine WFS1 cDNA, was constructed by the method described previously (31,32). AdCAGlacZ expressing β-galactosidase was used as a control adenovirus. Isolated islets were infected with the recombinant adenoviruses at 1.2×10^5 particles per islet in 1.0 ml medium for 60 min.

Isolation and static incubation of islets. Islets isolated from age-matched wild-type and mutant siblings at 14–17 weeks were isolated by retrograde injection of collagenase (Serva, Heidelberg, Germany) into the pancreatic duct according to standard procedures. For secretion studies, batches of 10 islets (triplicates for each condition) were kept in Krebs–Ringer-bicarbonate-HEPES buffer [KRBH; 140 mM NaCl, 3.6 mM KCl, 0.5 mM NaH_2PO_4, 0.5 mM $MgSO_4$, 1.5 mM $CaCl_2$, 2 mM $NaHCO_3$, 10 mM HEPES (pH 7.4)] containing 0.1% BSA and stimulators indicated. Islet insulin content was measured following extraction by acid ethanol. Insulin was detected by radioimmunoassay.

Single cell Ca^{2+} measurement. Islets isolated from mice at 12–16 weeks were dispersed, plated on glass-bottomed dishes and cultured for 3 days before measurement. β-Cells were identified by adenovirus-mediated expression of green fluorescent protein driven by the insulin promoter (33). We performed experiments without adenovirus-mediated expression of green fluorescent protein, identifying β-cells with immunostaining after perfusion, and observed similar results (data not shown). Cells were incubated with 1 μM Fura 2-AM (Dojindo, Kumamoto, Japan) for 30 min, perfused with KRBH and excited at 340 and 380 nm. A cooled CCD camera (Hamamatsu Photonics, Shizuoka, Japan) mounted on a microscope (Leica Microsystems, Heerbrugg, Switzerland) was used to capture fluorescence images. Ca^{2+} rises were compared by calculating areas between Ca^{2+} curves and baselines for the 300 s after the onset of Ca^{2+} rises.

LM-PCR amplification of DNA fragments. Groups of 50 islets isolated from mice at 15–17 weeks of age were cultured for 3 days in RPMI with different glucose concentrations. In another series of experiments, groups of 50 islets were treated with 2 μg/ml tunicamycin (Sigma-Aldrich Japan), 2 μM thapsigargin (Alamone Labs, Jerusalem, Israel) or a combination of interferon-γ (100 units/ml; PeproTech, London, UK) and tumor necrosis factor-α (500 units/ml; PeproTech). Genomic DNA was isolated from treated islets using the DNeasy kit (Qiagen-Japan, Tokyo, Japan). The PicoGreen® dsDNA quantitation kit (Molecular Probes, Eugene, OR, USA) was used to determine the DNA concentrations. 200 ng of the genomic DNA was ligated with an adaptor, which has been generated by annealing two synthetic oligonucleotides 5′-AGCACTCTCGAGCCTCT CACCGCA-3′ and 5′-TGCGGTGAGAGG-3′. A portion of ligation mixture (30%) was used for the PCR amplification with a primer 5′-AGCACTCTCGAGCCTCTCACCGCA-3′. The resulting PCR products were run on 1.2% agarose gels. Intensities of ladders between 500 and 1000 bp were analyzed using the Scion Image software. In order to compare data from separate gels, band intensity was normalized to the average laddering of the control islets at 5 mM glucose.

Statistical analyses

Data are presented as mean ± SE, unless otherwise noted. Differences between wild-type and mutant animals were assessed by Student's *t*-test.

ACKNOWLEDGEMENTS

We thank Professor H. Takeshima, Dr Y. Ohwada and Professor T. Itoh, Tohoku University, for their help in Ca^{2+} imaging and immunohistochemical analyses. We are also grateful to N. Nishino, T. Wadatsu and N. Miyazawa, Otsuka GEN Research Institute, for their help in generation of WFS1-deficient mice. Y. Takahashi is gratefully acknowledged for her excellent technical assistance. This study was supported by Grants in Aid for Scientific Research (13204062) to Y.O. from the Ministry of Education, Science, Sports and Culture of Japan.

REFERENCES

1. Wolfram, D.J. and Wagener, H.P. (1938) Diabetes mellitus and simple optic atrophy among siblings: report on four cases. *Mayo Clinic Proc.*, **13**, 715–718.
2. Swift, M. and Swift, R.G. (2001) Psychiatric disorders and mutations at the Wolfram syndrome locus. *Biol. Psychiatry*, **47**, 787–793.
3. Inoue, H., Tanizawa, Y., Wasson, J., Behn, P., Kalidas, K., Bernal-Mizrachi, E., Mueckler, M., Marshall, H., Donis-Keller, H., Crock, P. *et al.* (1998) A gene encoding a transmembrane protein is mutated in patients with diabetes mellitus and optic atrophy (Wolfram syndrome). *Nat. Genet.*, **20**, 143–148.
4. Strom, T.M., Hoetnagael, K., Hofmann, S., Gekeler, F., Scharfe, C., Rabl, W., Gerbitz, K.D. and Meitinger, T. (1998) Diabetes insipidus, diabetes mellitus, optic atrophy and deafness (DIDMOAD) caused by mutations in a novel gene (wilframin) coding for a predicted transmembrane protein. *Hum. Mol. Genet.*, **7**, 2021–2028.
5. Cryns, K., Sivakumaran, T.A., Van den Ouweland, J.M., Pennings, R.J., Cremers, C.W., Flothmann, K., Young, T.L., Smith, R.J., Lesperance, M.M. and Van Camp, G. (2003) Mutational spectrum of the *WFS1* gene in Wolfram syndrome, nonsyndromic hearing impairment, diabetes mellitus, and psychiatric disease. *Hum. Mut.*, **22**, 275–287.
6. Bespalova, I.N., Van Camp, G., Bom, S.J., Brown, D.J., Cryns, K., DeWan, A.T., Erson, A.E., Flothmann, K., Kunst, H.P., Kurnool, P. *et al.* (2001) Mutations in the Wolfram syndrome 1 gene (WFS1) are a common cause of low frequency sensorineural hearing loss. *Hum. Mol. Genet.*, **15**, 2501–2508.
7. Young, T.L., Ives, E., Lynch, E., Person, R., Snook, S., MacLaren, L., Cater, T., Griffin, A., Fernandez, B., Lee, M.K. *et al.* (2001) Non-syndromic progressive hearing loss DFNA38 is caused by heterozygous missense mutation in the Wolfram syndrome gene *WFS1*. *Hum. Mol. Genet.*, **15**, 2509–2514.
8. Ohta, T., Koizumi, A., Kayo, T., Shoji, Y., Watanabe, A, Monoh, K., Higashi, K., Ito, S., Ogawa, O., Wada, Y. *et al.* (1998) Evidence of an increased risk of hearing loss in heterozygous carriers in a Wolfram syndrome family. *Hum. Genet.*, **103**, 470–474.
9. Minton, J.A., Hattersley, A.T., Owen, K., McCarthy, M.I., Walker, M., Latif, F., Barrett, T. and Frayling, T.M. (2002) Association studies of genetic variation in the *WFS1* gene and type 2 diabetes in U.K. populations. *Diabetes*, **51**, 1287–1290.
10. Awata, T., Inoue, K., Kurihara, S., Ohkubo, T., Inoue, I., Abe, T., Takino, H., Kanazawa, Y. and Katayama, S. (2000) Missense variations of the gene responsible for Wolfram syndrome (WFS1/wolframin) in Japanese: possible contribution of the Arg456His mutation to type 1 diabetes as a nonautoimmune genetic basis. *Biochem. Biophys. Res. Commun.*, **268**, 612–616.
11. Sequeira, A. Kim, C., Seguin, M., Lesage, A., Chawky, N., Desautels, A., Tousignant, M., Vanier, C., Lipp, O., Benkelfat, C. *et al.* (2003) Wolfram syndrome and suicide: evidence for a role of WFS1 in suicidal and impulsive behavior. *Am. J. Mol. Genet.*, **119B**, 108–113.
12. Takeda, K., Inoue, H., Tanizawa, Y., Matsuzaki, Y., Oba, J., Watanabe, Y., Shinoda, K. and Oka, Y. (2001) WFS1 (Wolfram syndrome 1) gene product: predominant subcellular localization to endoplasmic reticulum in cultured cells and neuronal expression in rat brain. *Hum. Mol. Genet.*, **10**, 477–484.
13. Hofmann, S., Philbrook, C., Gerbitz, K.D. and Bauer, M.F. (2003) Wolfram syndrome: structural and functional analyses of mutant and wild-type wolframin, the WFS1 gene product. *Hum. Mol. Genet.*, **12**, 2003–2012.

14. Kaufmann, R. (2002) Orchestrating the unfolded protein response in health and disease. *J. Clin. Invest.*, **110**, 1389–1398.
15. Harding, H.P. and Ron, D. (2002) Endoplasmic reticulum stress and the development of diabetes. *Diabetes*, **51** (Suppl. 3), S455–S461.
16. Rando, T.A., Horton, J.C. and Layzer, R.B. (1992) Wolfram syndrome: evidence of a diffuse neurodegenerative disease by magnetic resonance imaging. *Neurology*, **42**, 1220–1224.
17. Karasik, A., O'Hara, C., Srikanta, S., Swift, M., Soeldner, J.S., Kahn, C.R. and Herskowitz, R.D. (1989) Genetically programmed selective islet beta-cell loss in diabetic subjects with Wolfram's syndrome. *Diabetes Care*, **12**, 135–138.
18. Ferri, K.F. and Koemer, G. (2001) Organelle-specific initiation of cell death pathways. *Nat. Cell Biol.*, **3**, E255–E263.
19. Coleman, D.L. (1982) Diabetes–obesity syndromes in mice. *Diabetes*, **31** (Suppl. 2), 1–6.
20. Terauchi, Y., Matsui, J., Suzuki, R., Kubota, N., Komeda, K., Aizawa, S., Eto, K., Kimura, S., Nagai, R., Tobe, K. *et al.* (2003) Impact of genetic background and ablation of insulin receptor substrate (IRS)-3 on IRS-2 knock-out mice. *J. Biol. Chem.*, **278**, 14284–14290.
21. Ishihara, H., Tashiro, F., Ikuta, K., Asano, T., Katagiri, H., Inukai, K., Kikuchi, M., Yazaki, Y., Oka, Y. and Miyazaki, J. (1995) Inhibition of pancreatic beta-cell glucokinase by antisense RNA expression in transgenic mice: mouse strain-dependent alteration of glucose tolerance. *FEBS Lett.*, **371**, 329–332.
22. Kulkarni, R.N., Almind, K., Goren, H.J., Winnay, J.N., Ueki, K., Okada, T. and Kahn, C.R. (2003) Impact of genetic background on development of hyperinsulinemia and diabetes in insulin receptor/insulin receptor substrate-1 double heterozygous mice. *Diabetes*, **52**, 1528–1534.
23. Wier, G.C., Bonner-Wier, S. and Leahy, J.L. (1990) Islet mass and function in diabetes and transplantation. *Diabetes*, **39**, 401–405.
24. Osman, A.A., Saito, M., Makepeace, C, Permutt, M.A., Schlesinger, P. and Mueckler, M. (2003) Wolframin expression induces novel ion channel activity in endoplasmic reticulum membranes and increases intracellular calcium. *J. Biol. Chem.*, **278**, 52755–52762.
25. Reddy, S. Bradley, J., Ginn, S., Pathipati, P. and Ross, J.M. (2003) Immunohistochemical study of caspase-3-expressing cells within the pancreas of non-obese diabetic mice during cyclophosphamide-accelerated diabetes. *Histochem. Cell Biol.*, **119**, 451–461.
26. Donath, M.Y., Gross, D.J., Cerasi, E. and Kaiser, N. (1999) Hyperglycemia-induced beta-cell apoptosis in pancreatic islets of *Psammomys obesus* during development of diabetes. *Diabetes*, **48**, 738–744.
27. Maedler, K., Sergeev, P., Ris, F., Oberholzer, J., Joller-Jemelka, H.I., Spinas, G.A., Kaiser, N., Halban, P.A. and Donath, M.Y. (2002) Glucose-induced beta cell production of IL-1beta contributes to glucotoxicity in human pancreatic islets. *J. Clin. Invest.*, **110**, 851–860.
28. Harding, H.P., Zeng, H., Xhang, Y., Jungries, R., Chung, P., Plesken, H., Sabatini, D.D. and Ron, D. (2001) Diabetes mellitus and exocrine pancreatic dysfunction in *Perk*$^{-/-}$ mice reveals a role for translational control in secretory cell survival. *Mol. Cell*, **7**, 1153–1163.
29. Butler, A.E., Janson, J., Bonner-Weir, S., Ritzel, R., Rizza, R.A. and Butler, P.C. (2003) β-Cell deficit and increased β-cell apoptosis in humans with type 2 diabetes. *Diabetes*, **52**, 102–110.
30. Cryns, K., Thys, S., van Laer, L., Oka, Y., Pfister, M., van Nassauw, L., Smith, R.J.H., Timmermans, J.P. and Van Camp, G. (2003) The *WFS1* gene, responsible for low frequent sensorineural hearing loss and Wolfram syndrome, is expressed in a variety of inner ear cells. *Histochem. Cell Biol.*, **119**, 247–256.
31. Miyake, S., Makimura, M., Kanegae, Y., Harada, S., Sato, Y., Takamori, K., Tokuda, C. and Saito, I. (1996) Efficient generation of recombinant adenoviruses using adenovirus DNA–terminal protein complex and a cosmid bearing the full-length virus genome. *Proc. Natl Acad. Sci. USA*, **93**, 1320–1324.
32. Niwa, H., Yamamura, K. and Miyazaki, J. (1991) Efficient selection for high-expression transfectants with a novel eukaryotic vector. *Gene*, **108**, 193–199.
33. Ishihara, H., Maechler, P., Gjinovci, A., Herrera, P.-L. and Wollheim, C.B. (2003) Islet β-cell secretion determines glucagon secretion from the neighboring α-cells. *Nat. Cell Biol.*, **5**, 330–335.

Available online at www.sciencedirect.com
SCIENCE DIRECT®
Peptides 25 (2004) 1803–1808
PEPTIDES
www.elsevier.com/locate/peptides

Genetic variations at urotensin II and urotensin II receptor genes and risk of type 2 diabetes mellitus in Japanese

Susumu Suzuki[a,*], Zong Wenyi[a], Masashi Hirai[a], Yoshinori Hinokio[a], Chitose Suzuki[a], Takahiro Yamada[a], Shinsuke Yoshizumi[a], Michiko Suzuki[b], Yukio Tanizawa[c], Akira Matsutani[c], Yoshitomo Oka[a]

[a] *Division of Molecular Metabolism and Diabetes, Department of Internal Medicine, Tohoku University Graduate School of Medicine, Sendai 980-8574, Japan*
[b] *Faculty of Comprehensive Human Science, Shokei Gakuin College, Natori 981-1295, Japan*
[c] *Division of Molecular Analysis of Human Disorders, Department of Bio-Signal Analysis, Yamaguchi University Graduate School of Medicine, Ube, Japan*

Received 1 March 2004; accepted 24 March 2004
Available online 15 September 2004

Abstract

Urotensin II is among the most potent vasoactive hormones known and the urotensin II (UTS2) gene is localized to 1p36-p32, one of the regions reported to show possible linkage with type 2 diabetes in Japanese. When we surveyed genetic polymorphisms in the UTS2 and urotensin II receptor (GPR14) gene, we identified two SNPs with amino acid substitutions (designated T21M and S89N and an SNP in the promotor region (−605G>A) of the UTS2 gene, and two SNPs in the non-coding region of the GPR14 gene. We then studied these three SNPs in the UTS2 gene and two SNPs in the GPR14 gene in 152 Japanese subjects with type 2 diabetes mellitus and two control Japanese populations. The allele frequency of 89N was significantly higher in type 2 diabetic patients than in both elderly normal subjects ($P = 0.0018$) and subjects with normal glucose tolerance ($P = 0.0011$), whereas the allele frequency of T21M and −605G>A in the UTS2 gene and those of two SNPs in the GPR14 gene were essentially identical in these three groups. Furthermore, in the subjects with normal glucose tolerance, 89N was associated with significantly higher insulin levels on oral glucose tolerance test, suggesting reduced insulin sensitivity in subjects with 89N. These results strongly suggest that subjects with S89N in the UTS2 gene are more insulin-resistant and thus more susceptible to type 2 diabetes mellitus development.

Keywords: Urotensin II; Urotensin II receptor (GPR14); Single nucleotide polymorphism; Insulin resistance; Type 2 diabetes; Normal glucose tolerance

1. Introduction

Urotensin II is known to be most potent mammalian vasoconstrictor identified to date [1,4,7], exerting its biological effects via interaction with a member of a G-protein-coupled receptor superfamily, originally termed GPR14 [10,15,17].

The urotensin II (UTS2) gene is localized to 1p36-p32, one of the regions showing potential linkage with type 2 diabetes in Japanese affected sib-pairs [16]. The urotensin II receptor is a G-protein-coupled 7-transmembrane receptor, encoded in the GPR14 (G-protein-coupled receptor 14) gene located in 17q25.3 [10,15,17].

Type 2 diabetes is characterized by insulin resistance in insulin target tissues and impaired insulin secretion from pancreatic β-cells [6], both of which are caused by multiple genetic and environmental factors.

Recent evidence suggests that vascular factor dysfunction contributes to insulin resistance [2]. Plasma concentrations of

Abbreviations: SNP, single nucleotide polymorphism; OGTT, oral glucose tolerance test; NGT, normal glucose tolerance

* Corresponding author. Tel.: +81 22 717 7171; fax: +81 22 717 7177.
E-mail address: ssuzuki@int3.med.tohoku.ac.jp (S. Suzuki).

0196-9781/$ – see front matter © 2004 Elsevier Inc. All rights reserved.
doi:10.1016/j.peptides.2004.03.030

urotensin II was reported to be elevated in type 2 diabetic patients [20]. Urotensin II reportedly reduces glucose-induced insulin secretion in the perfused rat pancreas [19]. Urotensin II and its receptor may, therefore, contribute to the insulin-secretory defects and/or insulin resistance in type 2 diabetes.

We investigated genetic polymorphisms in the UTS2 [21] and GPR14 genes. We demonstrated a significant association between one SNP in the UTS2 gene and the prevalence of type 2 diabetes in Japanese. Further analysis suggested this SNP to be associated with insulin resistance. The possible contribution of the UTS2 gene to the pathogenesis of type 2 diabetes is discussed herein.

2. Subjects and methods

2.1. Subjects

We employed two control Japanese populations, as described previously [21]. One consisted of 122 elderly subjects who met stringent criteria for normal: 60 or more years of age, no past history of diabetes, hemoglobin A1c (HbA1c) less than 5.6%, and no third degree or closer relatives with diabetes. Applying these criteria reduced the possibility of including subjects who would later develop diabetes. Another consisted of 268 subjects undergoing routine annual health examinations and showing normal glucose tolerance (NGT) by 75 g oral glucose tolerance test (OGTT) using the WHO criteria. One hundred and fifty-two unrelated patients with type 2 diabetes were randomly recruited from the outpatient clinic of Tohoku University Hospital. Type 2 diabetes was diagnosed using the WHO criteria. The study protocol and genetic analysis of human subjects were reviewed and approved by the Tohoku University Institutional Review Board. Appropriate informed consent was obtained from all subjects examined, including the elderly control subjects and the NGT subjects. The insulin sensitivity index, HOMA(R), in the NGT subjects was assessed using the HOMA model [14]. ISI composite [13], another insulin sensitivity index, was calculated from plasma glucose and insulin concentrations during OGTT. Clinical characteristics of the elderly control subjects, NGT subjects, and type 2 diabetic patients are described previously [21].

2.2. Genomic DNA amplification and SNP identification

DNA was isolated from peripheral blood cells using a QIAamp DNA Mini Kit (QIAGEN, Hilden, Germany). To amplify coding regions and intron–exon boundaries from genomic DNA, a primer set was developed using the genomic sequence for UTS2. PCR was performed and each PCR fragment was directly sequenced in both directions (ABI PRISM 7700, PE Applied Biosystems, Mississauga, Canada). To screen for variants in UTS2, we sequenced the genomic DNA from 30 unrelated subjects with type 2 diabetes and that from 30 elderly control subjects.

2.3. SNP genotyping by PCR-RFLP

PCR-RFLP was employed to examine three SNPs in the UTS2 gene [12]. The nucleotide transition from C to T in codon 61 of the UTS2 gene, which results in amino acid transition from Thr to Met at amino acid position 21, generates an Hsp92 II site. This SNP was designated T21M for this study. The nucleotide transition from G to A in codon 266 (amino acid transition from Ser to Asp at amino acid position 89) eliminates an AfaI site. This SNP was designated S89N. SNP determination using PCR-RFLP was described previously [21].

2.4. SNP genotyping by hybridization probe assay on LightCycler

We used a hybridization probe assay on LightCycler to detect two SNPs in the GPR14 gene. Two fluorescent-labeled hybridization probes were designed for the simultaneous detection of the SNPs and detection of the variant alleles was performed by the melting curve analysis [11]. Two SNPs were detected with a single thermocycle protocol within 40 min. This method is rapid, highly sensitive, and high-throughput, and is thus suitable for routine clinical use and large-scale studies. The hybridization probes were designed according to guidelines recommended by Roche Diagnostics, Inc. The mutation probe was designed so that the investigated mutation is under the probe. The anchor probe was designed to probe within the 1–5 nucleotides. The melting temperature (T_m) of the mutation probe was designed to be approximately 5 °C lower than that of the anchor probe. The 5′-end of the probe placed downstream of the other probe was labeled with LC Red 640 and the 3′-end was phosphorylated. The 3′-end of the other probe was labeled by FITC. The primers and hybridization probes were synthesized by Nihon Gene Research Laboratories, Inc. (Sendai, Japan). All PCR condition used 4 mM $MgCl_2$, 0.5 μM of the two PCR primers each, 0.4 μM LC Red 640 labeled hybridization probes, 2 μl of LightCycler DNA Master Hybridization Mix (Roche, Mannheim, Germany) and 5–30 ng DNA in a final volume of 20 μl. The fluorometer gain setting was 20 in channel 2. The cycling program consisted of 15 s of initial denaturation at 95 °C and 40 cycles at 95 °C for 0 s (ramp rate 20 °C/s), 60 °C for 15 s (ramp rate 3.0 °C/s), and 72 °C for 9 s (ramp rate 20 °C/s). The analytical melting program was 95 °C for 20 s and 40 °C for 120 s, increasing to 85 °C at a ramp rate of 0.1 °C/s, with continuous fluorescence acquisition.

2.5. Statistical analysis

The association of SNP genotypes with diabetes was assessed by an analysis of contingency tables. Fisher's exact test was used to compare differences in proportions between groups. Pair-wise *t*-tests were used to compare differences in the least-squares means of quantitative traits between groups. Statistical analyses were performed using the statistical anal-

ysis package of SPSS (Statistical Package for the Social Sciences).

3. Results

3.1. UTS2

We identified two major SNPs with amino acid substitutions (designated T21M and S89N) and one major SNP in the promotor region (−605G>A) in the UTS2 gene, in Japanese control subjects and type 2 diabetic patients. Fig. 1 demonstrates the genetic structure and all genetic polymorphisms detected in the UTS2 gene in Japanese. The allelic frequency of other SNPs except these three SNPs was not so frequent.

A case–control study was performed by comparing the allele frequencies of UTS2 gene SNPs in 122 elderly control subjects, 268 NGT subjects, and 152 unrelated subjects with type 2 diabetes. The genetic frequency of SNP for Asn at amino acid 89 of prourotensin II was significantly higher in type 2 diabetic patients than in the elderly control subjects ($P = 0.0042$), as shown in Table 1 [21]. These elderly controls are expected to be "supernormal" in terms of having diabetogenic genes, since they met very stringent criteria: 60 or more years of age, no past history of diabetes, HbA1c less than 5.6%, and no third degree or closer relatives with diabetes. A highly significant difference in the genotype frequency of SNP-S89N was noted when type 2 diabetic patients were compared to the other controls, the NGT subjects ($P = 0.0005$). These findings were confirmed when allele frequencies were compared. The allele frequency of 89N was significantly higher in type 2 diabetic patients than in the elderly controls ($P = 0.0018$) and NGT ($P = 0.0011$) subjects. In contrast to the SNP-S89N findings, no difference in T21M-SNP was observed; the allele frequency of 21M was essentially identical in type 2 diabetic patients (36%), the elderly controls (34%) and NGT subjects (35%) (data not shown). There was no difference in the allelic or genotypic distribution of −605G>A between type 2 diabetic patients and the elderly control subjects (data not shown). There was no deviation of observed genotype frequencies from the Hardy-Weinberg expectation.

Table 1
Genotype and allele frequency of S89N in elderly controls, normal glucose tolerance (NGT) subjects, and type 2 diabetic patients

	Elderly controls	NGT	Type 2 diabetes
SNP-89 genotype			
Asn/Asn	3 (2.4%)	16 (6.0%)	11 (7.2%)
Ser/Asn	38 (31.2%)	74 (27.6%)	69 (45.4%)
Ser/Ser	81 (66.4%)	178 (66.4%)	72 (47.4%)
Sum	122	268	152
P-value	0.0042	0.0005	
SNP-89 allele			
Asn	44 (18.0%)	106 (19.8%)	91 (29.9%)
Ser	200 (82.0%)	430 (80.2%)	213 (70.1%)
Sum	244	536	304
χ_c^2	9.70	10.6	
P_c-value	0.0018	0.0011	
Odds ratio	1.94	1.73	

Means ± S.D. (vs. type 2 diabetes). Reproduced from [21] with permission from Springer-Verlag, Heidelberg.

The NGT subjects undergoing routine annual health examinations at Shimonoseki Kosei Hospital had their plasma insulin levels measured before and during OGTT. We therefore further studied the possible association of S89N with insulin sensitivity and/or insulin-secretory capacity in these NGT subjects ($n = 101$). The NGT subjects with the 89N allele had significantly elevated plasma insulin concentrations at 0 and 120 min and higher plasma glucose levels at 120 min of OGTT (Table 2). Their ∑PG, ∑PI (summations of plasma glucose and insulin levels during OGTT, respectively) and HbA1c values were also significantly greater than those of subjects with the 89S allele. It is noteworthy that the differences are small, as expected in NGT subjects, but statistically significant. Thus, even in NGT subjects, subjects with the 89N allele have minimally elevated plasma glucose, accompanied by slightly elevated plasma insulin, suggesting that the 89N allele contributes to insulin resistance. Indeed, HOMA(R) of NGT subjects with the 89N allele was significantly higher than that of subjects with the 89S allele ($P =$

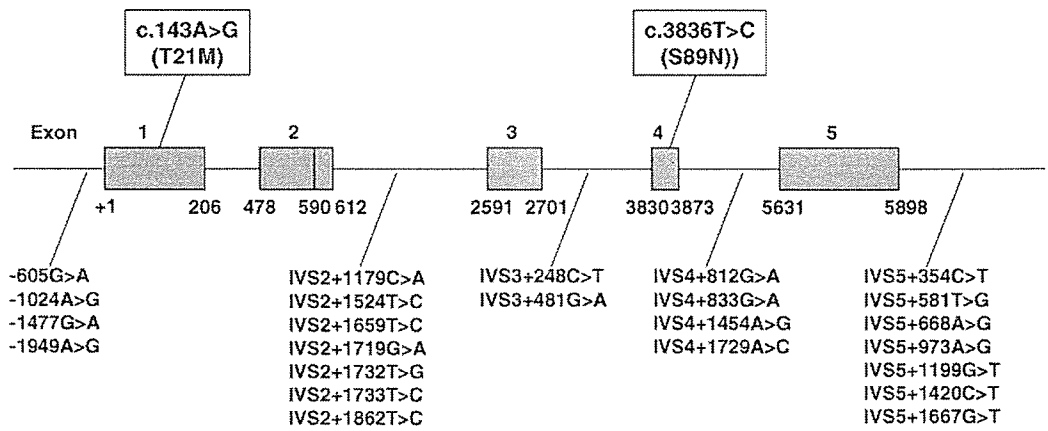

Fig. 1. Genetic polymorphisms in the urotensin II (UTS2) gene in Japanese. IVS: intervening sequence.

Table 2
Metabolic parameters in normal glucose tolerance (NGT) subjects classified according to S89N genotypes or alleles

Codon 89	*N*	IRI 0	IRI 120	∑BS	∑IRI	HOMA(R)	ISI composite
Asn/Asn	10	8.56 ± 2.24	43.9 ± 20.9	664 ± 104	212 ± 107	2.04 ± 0.58	3.09 ± 0.67
Ser/Asn	31	7.32 ± 2.30	35.5 ± 20.9	629 ± 95	167 ± 74	1.78 ± 0.58	3.48 ± 0.82
Ser/Ser	60	6.74 ± 1.70	28.1 ± 15.1	595 ± 79	150 ± 64	1.62 ± 0.46	3.75 ± 0.70
P (Asn/Asn vs. Ser/Ser)	0.0039	0.0051	0.017	0.014	0.0122	0.0071	
Asn	51	7.81 ± 2.31	38.8 ± 20.9	643 ± 98	185 ± 89	1.88 ± 0.58	3.33 ± 0.77
Ser	151	6.86 ± 1.74	29.6 ± 16.6	602 ± 83	154 ± 66	1.65 ± 0.49	3.70 ± 0.73
P (Asn vs. Ser)	0.0032	0.0016	0.0041	0.0089	0.0063	0.0023	

Means ± S.D. Adapted from [21] with permission from Springer-Verlag, Heidelberg.

0.0063). NGT subjects with the 89N allele had significantly lower ISI composite values than NGT subjects with the 89S allele ($P = 0.0023$). These data indicate that the 89N allele is associated with an insulin-resistant phenotype in NGT subjects. In contrast to SNP-S89N, the values described above are essentially identical in subjects with the 21T allele and those with the 21M allele (data not shown). There were also no association between the NGT subjects with −605G and the subjects with −605A (data not shown).

3.2. GPR14

The GPR14 gene is composed of a single large exon expanding to 1.17 kb, as shown in Fig. 2. We could not identify any SNP in the coding region of the GPR14 gene. We only found two major SNPs in the non-coding regions of GPR14 gene, designated −7836A/G and −7814C/T, in Japanese elderly control subjects and type 2 diabetic patients. A case–control study was performed by comparing the allele frequencies of the SNPs in 147 elderly control subjects and 155 unrelated subjects with type 2 diabetes. There were no difference in the genotypes or alleles of −7836A/G or −7814C/T; the allele frequency of −7836A/G or −7814C/T was essentially identical in type 2 diabetic patients and the elderly controls (Table 3). There was no deviation of observed genotype frequencies from the Hardy-Weinberg expectation.

The clinical parameter values are essentially identical in subjects with the −7836A allele and with the −7836G alleles. The values described above are essentially identical in subjects with or without −7814C/T (not shown).

Table 3
Genotype and allele frequencies of SNPs of the GPR14 gene in supernormal, and type 2 diabetic patients

	Elderly controls	DM
−7836A/G		
G/G	59 (49.6%)	58 (45.7%)
G/A	54 (45.4%)	57 (44.9%)
A/A	6 (5.0%)	12 (9.4%)
Sum	119	127
P-value	NS	
G	172 (72.3%)	173 (68.1%)
A	66 (27.7%)	81 (31.9%)
Sum	238	254
χ_c^2	0.825	
P_c-value	NS	
Odds ratio	1.22	
−7814C/T		
T/T	13 (8.8%)	16 (10.3%)
T/C	60 (40.8%)	65 (41.9%)
C/C	74 (50.3%)	74 (47.7%)
Sum	147	155
P-value	NS	
T	86 (29.3%)	97 (31.3%)
C	208 (70.7%)	213 (68.7%)
Sum	294	310
χ_c^2	0.208	
P_c-value	NS	
Odds ratio	0.91	

Means ± S.D. (vs. type 2 diabetes).

4. Discussion

This case–control association demonstrates a highly statistically significant difference in SNP-S89N frequency between the subjects with type 2 diabetes and the two control Japanese populations: *P*-values of allele frequency difference were 0.0018 versus the elderly controls and 0.0011 versus the NGT subjects [21]. Involvement of SNP-S89N in the development of diabetes was further supported by the results obtained in NGT subjects. Effects of SNP-S89N on glucose metabolism were evident even in NGT subjects. Plasma glucose appears to be slightly elevated in NGT subjects with the 89N allele as compared to those with the 89S allele, as demonstrated by higher glucose levels at 120 min of OGTT and higher HbA1c levels in NGT subjects with the 89N allele.

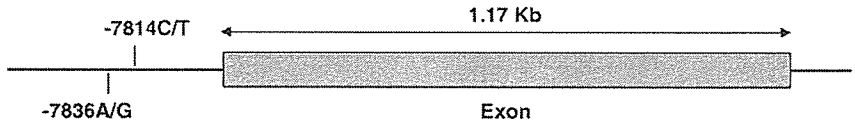

Fig. 2. Genetic polymorphisms in the urotensin II receptor (GPR14) gene in Japanese.

It is noteworthy that plasma insulin levels while fasting (time 0) and at 120 min of OGTT were also greater in those with the 89N allele than in those with the 89S allele. HOMA(R), which is calculated from fasting plasma glucose and insulin levels, is significantly greater in those with the 89N allele. These results strongly suggest that subjects with the 89N allele are more insulin-resistant than those with the 89S allele, and are thus more likely to develop diabetes.

The UTS2 gene is localized to 1p36, one of the regions showing potential linkage with type 2 diabetes in Japanese affected sib-pairs [16]. Linkage of this region with type 2 diabetes in Chinese and higher prevalence of the 89N allele in Chinese subjects with type 2 diabetes were recently reported in abstract form [9]. Our findings in the present case–control study are consistent with the report on Chinese subjects. Furthermore, the present study analyzing NGT subjects provides evidence that the 89N allele is associated with insulin resistance in Japanese. It would be of interest to determine whether SNP-S89N is associated with insulin resistance in other ethnic groups including Chinese.

Urotensin II is known to be most potent mammalian vasoconstrictor identified to date [1,4,7], exerting its biological effects via interaction with a member of a G-protein-coupled receptor superfamily, originally termed GPR14 [10,15,17]. Insulin induces endothelial-nitric-oxide-dependent vasodilatation. Recent data suggest that insulin's metabolic and vascular actions are closely linked [2]. Indeed, insulin-resistant states are associated with diminished insulin-mediated glucose uptake into peripheral tissues, and impaired insulin-mediated vasodilatation as well as impaired endothelium-dependent vasodilatation in response to the muscarinic receptor agonist acetylcholine. Several vasoactive hormones including endothelin-1 modulate insulin-mediated vasodilatation and induce insulin resistance in peripheral tissues and endothelium [2]. The present study is the first to show that SNP of the gene for the vasoactive hormone urotensin II contributes to insulin resistance.

Urotensin II may directly, rather than via vasoconstriction, affect glucose metabolism. Since appreciable numbers of urotensin II receptors are present in human skeletal muscle [12], urotensin II may regulate insulin sensitivity in skeletal muscle. The expression of urotensin II in the human liver also suggests a possible role of urotensin II in hepatic glucose homeostasis. In fish, urotensin II administration decreased hepatic glycogen content and increased glucose-6-phosphatase activity in the liver [18]. Further studies are needed to clarify the possible role of urotensin II in insulin signaling. Urotensin II receptor knockout mice are currently established and provide a direct evidence that the signaling of urotensin II occurred through its specific receptor, GPR14 [3]. Breeding GPR14 knockout mice onto a genetic background of diabetes (db/db, ob/ob mice, etc.) may be a good method for determining the influence of urotensin II and its receptor on the etiology of type 2 diabetes mellitus.

Urotensin II exerts a broad spectrum of biological actions in mammals: responses that influence cardiovascular, renal, pulmonary, central nervous system and endocrine function. Thus, urotensin II is proposed to contribute to human diseases including atherosclerosis, cardiac hypertrophy, pulmonary hypertension, hypertension and diabetes. It is a first report that the SNP in urotensin II gene contributes to the pathogenesis of type 2 diabetes. Future investigation should conduct to elucidate whether the SNPs in UTS2 and GPR14 genes associate with these polygenetic diseases, such as atherosclerosis, cardiac hypertrophy, pulmonary hypertension, hypertension.

Urotensin II is a cyclic dodecapeptide, derived from two splice variants of preproprotein with 124 or 138 amino acids through proteolytic cleavage by putative polybasic endopeptidase [1,5,8]. There are no previous reports indicating that the amino acid transition from Ser to Asn at position 89 influences the post-translational processing of preprourotensin II. Future investigation should focus on whether S89N affects the processing and/or secretion of urotensin II.

In conclusion, our results strongly suggest that subjects with S89N in the UTS2 gene are more insulin-resistant and thus more susceptible to type 2 diabetes mellitus development. The UTS2 gene is among the diabetogenic genes in the Japanese population.

Acknowledgements

We are grateful to all the patients who participated in this study and to their referring physicians. We would also like to thank the elderly controls and NGT subjects for participating. This study was supported by Grants in Aid for Creative Basic Research (10NP0210) and for Scientific Research (13204062) to Y.O. and Grants in Aid for Scientific Research (70216399) to S.S. from the Ministry of Education, Science, Sports and Culture of Japan and Grants to S.S. from Japan Diabetes Foundation and Japan Science and Technology Corporation (CREST).

References

[1] Ames RS, Sarau HM, Chambers JK, Willette RN, Aiyar NV, Romanic AM, et al. Human urotensin-II is a potent vasoconstrictor and agonist for the orphan receptor GPR14. Nature 1999;401:282–6.
[2] Baron AD. Insulin resistance and vascular function. J Diabetes Complications 2002;16:92–102.
[3] Behm DJ, Harrison SM, Ao Z, Maniscalco K, Pickering SJ, Grau EV, et al. Deletion of the UT receptor gene results in the selective loss of urotensin-II contractile activity in aortae isolated from UT receptor knockout mice. Br J Pharmacol 2003;139:464–72.
[4] Bohm F, Pernow J. Urotensin II evokes potent vasoconstriction in humans in vivo. Br J Pharmacol 2002;135:25–7.
[5] Coulouarn Y, Lihrmann I, Jegou S, Anouar Y, Tostivint H, Beauvillain JC, et al. Cloning of the cDNA encoding the urotensin II precursor in frog and human reveals intense expression of the urotensin II gene in motoneurons of the spinal cord. Proc Natl Acad Sci USA 1998;95:15803–8.
[6] DeFranzo RA, Bonadonna RC, Ferrannini E. Pathogenesis of NIDDM: a balanced overview. Diabetes Care 1992;15:318–68.
[7] Douglas SA, Ohlstein EH. Human urotensin-II, the most potent mammalian vasoconstrictor identified to date, as a therapeutic target

for the management of cardiovascular disease. Trends Cardiovasc Med 2000;10:229–37.
[8] Elshourbagy NA, Douglas SA, Shabon U, Harrison S, Duddy G, Sechler JL, et al. Molecular and pharmacological characterization of genes encoding urotensin-II peptides and their cognate G-protein-coupled receptors from the mouse and monkey. Br J Pharmacol 2002;136:9–22.
[9] Ji L, Zhu F, Luo B. The role of urotensin II gene in the genetic susceptibility to type 2 diabetes in Chinese population. Diabetes 2002;51(Suppl 2):260.
[10] Liu Q, Pong SS, Zeng Z, Zhang Q, Howard AD, Williams Jr DL, et al. Identification of urotensin II as the endogenous ligand for the orphan G-protein-coupled receptor GPR14. Biochem Biophys Res Commun 1999;266:174–8.
[11] Lyon E. Mutation detection using fluorescent hybridization probes and melting curve analysis. Expert Rev Mol Diagn 2001;1:92–101.
[12] Maguire JJ, Kuc RE, Davenport AP. Vasoconstrictor activity of novel endothelin peptide, ET-1(1-31), in human mammary and coronary arteries in vitro. Br J Pharmacol 2001;134:1360–6.
[13] Matthews DR, Hosker JP, Rudenski AS, Naylor BA, Treacher DF, Turner RC. Homeostasis model assessment: insulin resistance and beta-cell function from fasting plasma glucose and insulin concentrations in man. Diabetologia 1985;28:412–9.
[14] Matsuda M, DeFronzo RA. Insulin sensitivity indices obtained from oral glucose tolerance testing: comparison with the euglycemic insulin clamp. Diabetes Care 1999;22:1462–70.
[15] Mori M, Sugo T, Abe M, Shimomura Y, Kurihara M, Kitada C, et al. Urotensin II is the endogenous ligand of a G-protein-coupled orphan receptor SENR (GPR14). Biochem Biophys Res Commun 1999;265:123–9.
[16] Mori Y, Otabe S, Dina C, Yasuda K, Populaire C, Lecoeur C, et al. Genome-wide search for type 2 diabetes in Japanese affected sib-pairs confirms susceptibility genes on 3q, 15q, and 20q and identifies two new candidate loci on 7p and 11p. Diabetes 2002;51:1247–55.
[17] Nothacker HP, Wang Z, McNeill AM, Saito Y, Merten S, O'Dowd B, et al. Identification of the natural ligand of an orphan G-protein-coupled receptor involved in the regulation of vasoconstriction. Nat Cell Biol 1999;1:383–5.
[18] Sheridan MA, Plisetskaya EM, Bern HA, Gorbman A. Effects of somatostatin-25 and urotensin II on lipid and carbohydrate metabolism of coho salmon *Oncorhynchus kisutch*. Gen Comp Endocrinol 1987;66:405–14.
[19] Silvestre RA, Rodriguez-Gallardo J, Egido EM, Marco J. Inhibition of insulin release by urotensin II – a study on the perfused rat pancreas. Horm Metab Res 2001;33:379–81.
[20] Totsune K, Takahashi K, Arihara Z, Sone M, Ito S, Murakami O. Increased plasma urotensin II levels in patients with diabetes mellitus. Clin Sci (London) 2003;104:1–5.
[21] Wenyi Z, Suzuki S, Hirai M, Hinokio Y, Tanizawa Y, Matsutani A, et al. Role of urotensin II gene in genetic susceptibility to type 2 diabetes mellitus in Japanese subjects. Diabetologia 2003;46:972–6.

Available online at www.sciencedirect.com
SCIENCE DIRECT®
Biochemical and Biophysical Research Communications 325 (2004) 250–256
BBRC
www.elsevier.com/locate/ybbrc

Endoplasmic reticulum stress and N-glycosylation modulate expression of WFS1 protein

Suguru Yamaguchi[a], Hisamitsu Ishihara[a,*], Akira Tamura[a], Takahiro Yamada[a], Rui Takahashi[a], Daisuke Takei[a], Hideki Katagiri[b], Yoshitomo Oka[a]

[a] *Division of Molecular Metabolism and Diabetes, Tohoku University Graduate School of Medicine, 2-1 Seiryo-machi, Aoba-ku, Sendai, Miyagi 980-8575, Japan*
[b] *Division of Advanced Therapeutics for Metabolic Diseases, Tohoku University Graduate School of Medicine, 2-1 Seiryo-machi, Aoba-ku, Sendai, Miyagi 980-8575, Japan*

Received 22 September 2004
Available online 22 October 2004

Abstract

Mutations of the *WFS1* gene are responsible for two hereditary diseases, Wolfram syndrome and low frequency sensorineural hearing loss. The WFS1 protein is a glycoprotein located in the endoplasmic reticulum (ER) membrane but its function is poorly understood. Herein we show WFS1 mRNA and protein levels in pancreatic islets to be increased with ER-stress inducers, thapsigargin and dithiothreitol. Another ER-stress inducer, the N-glycosylation inhibitor tunicamycin, also raised WFS1 mRNA but not protein levels. Site-directed mutagenesis showed both Asn-663 and Asn-748 to be N-glycosylated in mouse WFS1 protein. The glycosylation-defective WFS1 protein, in which Asn-663 and Asn-748 had been substituted with aspartate, exhibited an increased protein turnover rate. Consistent with this, the WFS1 protein was more rapidly degraded in the presence of tunicamycin. These data indicate that ER-stress and N-glycosylation play important roles in WFS1 expression and stability, and also suggest regulatory roles for this protein in ER-stress induced cell death.

Keywords: Wolfram syndrome; Low frequency sensorineural hearing loss; WFSI; ER-stress; N-Glycosylation

The *WFS1* gene, encoding a transmembrane protein of the endoplasmic reticulum (ER) [1], is mutated in two hereditary diseases, autosomal recessive Wolfram syndrome (OMIN:222300) [2,3] and autosomal dominant low frequency sensorineural hearing loss (LFSNHL) (OMIM:600965) [4,5]. The former is also known as DIDMOAD, summarizing the most frequent symptoms; diabetes insipidus, diabetes mellitus, optic atrophy, and deafness. More than 100 mutations of the *WFS1* gene have been identified to date in patients with these diseases [6]. WFS1 protein, also called wolframin, consists of 890 amino acids [2,3] and its homologues are found in several organisms; *Drosophila melanogaster* (CG4917), *Anopheles gambiae* (EBIP3764), *Ciona intestinalis* (Cin.16116), *Fugu rubripes* (SINFRUP82345), and *Xenopus laevis* (Xl.3995). However, these proteins share no homology with known proteins, making it difficult to speculate as to their functions.

We recently established a murine model with a disrupted *wfs1* gene [7]. Mutant mice exhibited impaired glucose homeostasis due to defective insulin secretion in vivo. Studies using isolated islets revealed that mutant islet cells were prone to apoptosis induced by insults which impair ER functions and trigger the so-called unfolded protein response (UPR) [8,9]. Therefore, it was suggested that WFS1 protein plays a role in modulation of apoptotic processes that arise from impairment of ER function [7]. In addition, isolated islets from WFS1-deficient mice exhibited defective insulin

* Corresponding author. Fax: +81 22 717 7612.
E-mail address: ishihara-tky@umin.ac.jp (H. Ishihara).

0006-291X/$ - see front matter © 2004 Elsevier Inc. All rights reserved.
doi:10.1016/j.bbrc.2004.10.017

secretion which was accompanied by decreased calcium responses to glucose. Conversely, wolframin-overexpressing islets showed increased insulin secretion, indicating that wolframin also participates in regulation of stimulus-secretion coupling in insulin exocytosis [7]. It has recently been reported that WFS1 protein/wolframin expression in *Xenopus* oocytes conferred cation channel activity and increased cytosolic calcium levels [10]. This observation is intriguing since intracellular calcium regulation plays important roles in modulating both apoptotic and exocytotic processes. Despite these advancements, however, little is known about the mechanisms by which WFS1 protein actually alters these processes.

To understand the role that WFS1 protein/wolframin plays in the regulation of apoptotic and exocytotic events as well as in other as yet unknown cellular processes, information on the structure and function of this protein must be obtained. The amino acid sequence suggests that WFS1 protein is a multi-membrane spanning protein with hydrophilic amino (N)- and carboxy (C)-terminal regions [2,3]. In addition, biochemical and immunocytochemical analyses showed WFS1 protein to be an ER membrane glycoprotein [1].

In the present studies, we first examined WFS1 protein expression after treatment with agents that trigger UPR. We found WFS1 mRNA and protein levels to be increased by thapsigargin or dithiothreitol (DTT). Treatment with tunicamycin, an inhibitor of N-glycosylation, also raised WFS1 mRNA levels, suggesting that UPR increases WFS1 mRNA levels. However, the WFS1 protein level is not increased by tunicamycin. Subsequent analyses demonstrated protein stability to be reduced in the glycosylation-defective WFS1 protein. These results contribute to further understanding of the functions of this enigmatic protein.

Materials and methods

Reagents and antibodies. Tunicamycin, thapsigargin, DTT, and anti-actin antibody were purchased from Sigma–Aldrich Japan (Tokyo, Japan). Anti-HA and anti-CHOP antibodies were obtained from Santa Cruz Biotechnology (Santa Cruz, CA). Anti-WFS1 N-terminus antibody was described previously [11].

Pancreatic islet isolation and treatment with ER-stress inducers. Pancreatic islets were isolated from male C57BL/6 mice by retrograde injection of collagenase (Sigma–Aldrich Japan, Tokyo, Japan) into the pancreatic duct. Approximately 100 (for Western blot analyses) or 200 (for RNA extraction) islets were treated with 2 μg/ml thapsigargin, 5 mM DTT, or 5 μM tunicamycin for 36 h in RPMI1640 medium. Total RNA was extracted using Isogen reagent (NipponGene, Toyama, Japan). Quantitative real-time PCR analysis for WFS1 mRNA levels was performed using primers, 5′-CTGGAAACTCAACCCCAAGA-3′ and 5′-TTGGATTCACTGCTGACGAG-3′.

Plasmids. pHA-mWFS1 encodes a fusion protein consisting of an initiator methionine, the HA epitope tag (YPYDVPDYA), and amino acids 2–890 of mouse WFS1 protein. To generate this plasmid, a fragment encoding a *Sal*I restriction site and amino acids 2–484 was amplified by PCR. Using the PCR method, pmWFS1-HA encoding mouse WFS1 protein with an HA tag between residues 830 and 831 was also generated. pHA-mWFS1(N633D) and pHA-mWFS1 (N748D), which encode HA-tagged WFS1 protein with a mutation of asparagine 633 to aspartate and asparagine 748 to aspartate, respectively, were generated using PCR-based mutagenesis on pHA-mWFS1. pHA-mWFS1(N633D/N748D) encoding a mutant protein with mutation of both asparagine residues was generated using pHA-mWFS1(N633D).

Cell culture and transient transfection. MIN6 [12] and COS7 cells were grown in Dulbecco's modified Eagle's medium (DMEM) supplemented with 10% (v/v) fetal calf serum, 50 U/ml penicillin, and 50 μg/ml streptomycin sulfate. Transfection of plasmids was carried out using FuGENE6 (Roche, Indianapolis, IN) diluted in OPTI media (Invitrogen, Carlsbad, CA). Cells were harvested for Western blot or proceeded to immunostaining analysis 36 h after transfection. Immunostaining was performed using anti-HA antibody and FITC-conjugated anti-mouse IgG (Jackson ImmunoResearch, West Grove, PA).

Trypsin treatment. COS7 cells transfected with either pHA-mWFS1 or pmWFS1-HA were homogenized in a buffer containing 270 mM sucrose, 2 mM EDTA, and 50 mM Hepes (pH 7.5). Cellular membranes were recovered by centrifuging the homogenate at 17,400*g* for 15 min. Membranes (100 μg) were then incubated with trypsin at various concentrations at 4 °C. After a 30 min incubation, homogenates were boiled and subjected to SDS/PAGE and Western blot analysis.

Endoglycosydase cleavage. COS7 cells transfected with either wild-type WFS1 cDNA or mutant constructs were dissolved in denaturing buffer (0.5% SDS, 1% β-mercaptoethanol), boiled for 10 min at 100 °C, then incubated at 37 °C for 1 h with endoglycosidase H (500 U), and subjected to electrophoresis on NuPAGE 3–8% Tris–acetate gel (Invitrogen).

Metabolic labeling. MIN6 cells were labeled with [^{35}S]methionine and [^{35}S]cysteine (100 μCi/ml; EXPRE^{35}S^{35}S labeling mix, Perkin–Elmer-New England Nuclear, Boston, MA) in DMEM with either methionine or cysteine in the presence or absence of 5 μg/ml tunicamycin for 3 h. Cells were then chased for different periods in complete medium with or without tunicamycin. COS7 cells transfected with pHA-mWFS1 or pHA-mWFS1(N633D/N748D) were also labeled with [^{35}S]methionine and [^{35}S]cysteine for 3 h. Cells were then chased for different periods in complete medium. MIN6 and COS7 cells were lysed in a buffer containing 100 mM NaCl, 0.5 mM EDTA, 20 mM Tris (pH 7.5), and 0.5% NP-40. Lysates were incubated with 10 μl protein A/G–Sepharose (Amersham Biosciences, Piscataway, NJ) for 2 h and then briefly centrifuged. The resulting supernatant was incubated with anti-WFS1 N-terminus or anti-HA antibodies overnight and then incubated with protein A/G–Sepharose for 2 h. The beads were washed three times and bound WFS1 proteins were eluted in SDS-sample buffer and subjected to SDS/PAGE (10%).

Statistical analyses. Data are presented as means ± SE. Differences were assessed by Student's *t* test.

Results and discussion

Effect of ER-stress inducers on WFS1 expression in pancreatic islets

We recently reported that WFS1-deficient islets exhibited increased susceptibility to apoptosis due to impaired ER function [7]. Therefore, in this study, we first determined WFS1 expression in isolated mouse pancreatic islets treated with the ER-stress inducers, thapsigargin, DTT, and tunicamycin. Thapsigargin is an inhibitor of the sarco(endo)plasmic reticulum Ca^{2+} pump and

depletes ER Ca^{2+}, which affects the functions of Ca^{2+}-dependent ER chaperone proteins. DTT and tunicamycin affect protein folding by disrupting disulfide bonds and inhibiting N-glycosylation, respectively. These compounds therefore cause mis-folding of proteins (ER-stress) and induce UPR [13]. As shown in Fig. 1, WFS1 protein expression was increased in islets treated with 2 μM thapsigargin (Fig. 1A) or 5 mM DTT (Fig. 1B) for 36 h. Greater than threefold increases in WFS1 mRNA levels were also observed by quantitative RT-PCR analyses in islets treated with these agents (data not shown). Another ER-stress inducer, tunicamycin (5 μg/ml), did not raise WFS1 protein levels in isolated islets (Fig. 1C). However, quantitative RT-PCR analyses revealed WFS1 mRNA levels to be increased by 72% in islets treated with tunicamycin (Fig. 1D). These data suggest that WFS1 mRNA expression increases in response to the ER-stress.

WFS1 protein has been shown to be a glycoprotein [1] like the inositol trisphosphate receptor, another ER membrane resident protein essential for cellular calcium homeostasis and signaling [14]. The unaltered WFS1 protein levels despite increased mRNA levels in islets treated with tunicamycin raise the possibility that inhibition of N-glycosylation affects WFS1 protein stability. To address this possibility, pancreatic β-cell derived MIN6 cells were labeled for 3 h with [^{35}S]methionine/cysteine and chased with unlabeled methionine and cysteine for different intervals in the continuous absence or presence of tunicamycin. As shown in Fig. 1E, WFS1 protein in tunicamycin-treated cells was more rapidly degraded, suggesting that inhibition of N-glycosylation reduces WFS1 protein stability.

Membrane topology of WFS1 protein

To study the roles of N-glycosylation more specifically, we first sought to determine N-glycosylation site(s) of WFS1 protein/wolframin. Since N-glycosylation occurs in the ER, it was prerequisite to know the membrane topology of this protein. The initial hydropathy plot studies did not provide a definitive answer; WFS1 protein contains 9 or 10 transmembrane segments, with long hydrophilic stretches on both the N- and the C-termini [2,3].

To localize the N- and the C-termini of WFS1 protein with respect to the ER membrane, we transiently expressed, in COS7 cells, mouse WFS1 protein tagged with an HA-epitope in either the N- or the C-terminal stretch (designated HA-mWFS1 or mWFS1-HA, respectively,

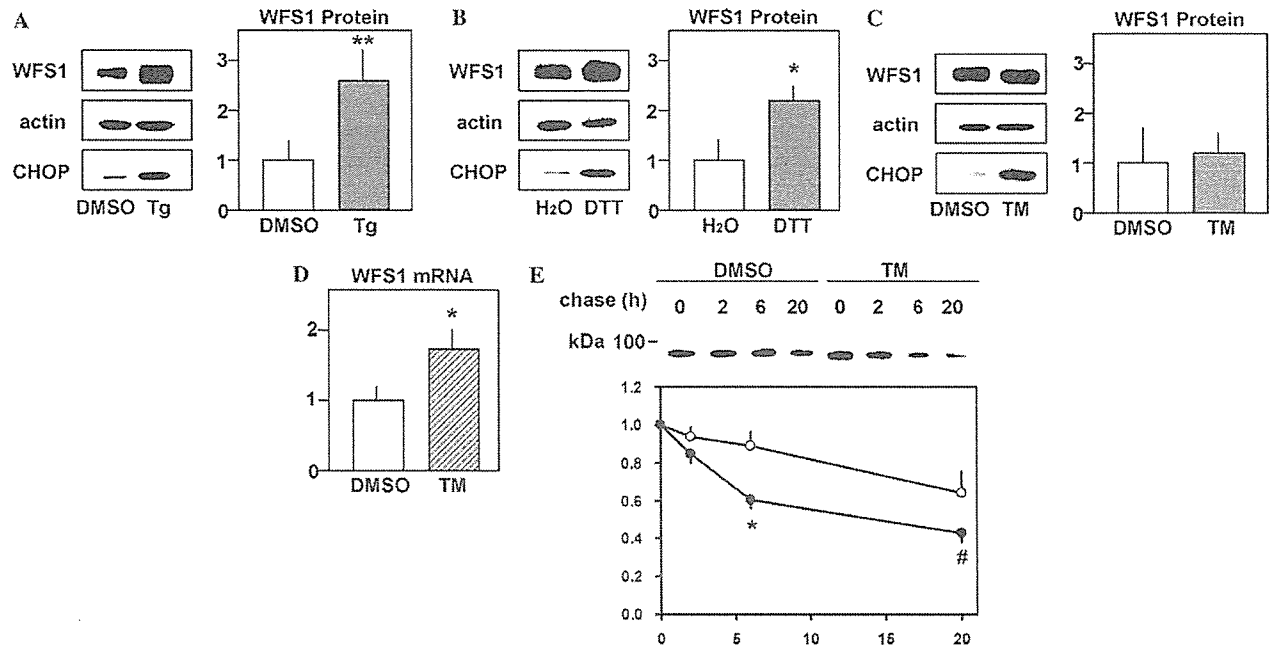

Fig. 1. WFS1 expression in mouse pancreatic islets in response to ER-stress inducers. (A–C) Isolated mouse islets were challenged with 2 μM thapsigargin (Tg) (A, $n = 4$), 5 mM DTT (B, $n = 3$) or 5 μg/ml tunicamycin (TM) (C, $n = 5$). After a 36-h incubation, the islets were subjected to SDS/PAGE and blotted using antibodies against the WFS1 N-terminus, actin, or CHOP. Representative blots are shown in the left panels. Increased CHOP expression indicated successful induction of ER-stress mediated apoptosis. WFS1 protein/actin levels are summarized in the right panels. Data are expressed as the expression relative to those of a control islet preparation. (D) Total RNA was extracted from isolated mouse islets treated with 5 μg/ml tunicamycin for 36 h. WFS1 and GAPDH mRNA levels were determined by quantitative real-time PCR. WFS1 mRNA levels were normalized to those of GAPDH. Data were obtained using three independent sets of islet preparations. (E) MIN6 cells were pulse-labeled for 3 h without or with 5 μg/ml tunicamycin and chased for up to 20 h in the continuous absence or presence of the drug. A representative result from three independent experiments is shown in the upper panel. Data from three experiments are summarized, after normalization to time zero of the chase in the lower panel. Open circles, DMSO-treated MIN6 cells. Closed circles, tunicamycin-treated cells. $^{\#}P = 0.0634$, $^{*}P < 0.05$, $^{**}P < 0.01$.

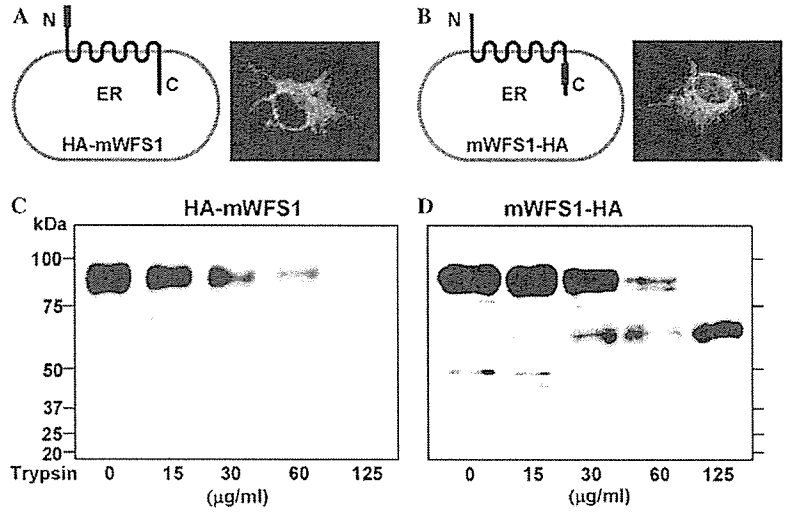

Fig. 2. Membrane orientations of the N- and the C-termini of WFS1 protein as determined by trypsin proteolysis. WFS1 protein tagged with the HA epitope at either the N- (A,C) or the C-terminus (B,D) was expressed in COS7 cells. (A,B) Schematic illustration and immunocytochemical demonstration of the HA-tagged WFS1 proteins used in (C) and (D). (C,D) Membranes from COS7 cells transfected with a plasmid encoding either HA-mWFS1 or mWFS1-HA were treated with the indicated amounts of trypsin. After incubation for 30 min at 4 °C, the reactions were stopped by boiling for 5 min, and subjected to SDS/PAGE and immunoblot analysis with anti-HA antibody.

Figs. 2A and B). HA-mWFS1 and mWFS1-HA proteins were successfully expressed and localized to the ER, as demonstrated by reticular staining in the cytoplasm (Figs. 2A and B). Membrane preparation of cells expressed with either HA-mWFS1 or mWFS1-HA proteins was then subjected to trypsin digestion followed by SDS/PAGE and immunoblotting with an antibody against the HA epitope. The HA-epitope tagged at the N-terminus was completely digested with increasing concentrations of trypsin (Fig. 2C). This was not due to loss of membrane vesicle integrity, since no changes in an ER-resident chaperone protein, GRP78, were detected using an antibody against GRP78 in the same membrane preparations (data not shown). In contrast, the C-terminal HA epitope was protected from trypsin (Fig. 2D). These results indicated that WFS1 protein has odd numbers of transmembrane segments with the orientation of the N-terminus toward the cytoplasm and that of the C-terminus toward the ER lumen. A similar conclusion was obtained by trypsin-digestion of the membrane, followed by detection with C-terminal or N-terminal antibodies [15].

Determination of N-glycosylation sites.

Mouse WFS1 protein has six asparagine residues with the consensus sequence for N-glycosylation (N-X-S/T, where X is any amino acid except for proline). According to a 9-transmembrane model with N-terminus cytosolic/C-terminus luminal orientation, asparagines 663 and 748 would be localized in the ER. Therefore, we mutated these two asparagine residues to aspartate in order to determine whether one or both are N-linked glycosylation site(s). Mutant WFS1 proteins in which asparagine 663 and/or asparagine 748 was mutated to aspartate [designated HA-mWFS1(N663D), HA-mWFS1(N748D), and HA-mWFS1(N663D/N748D)] were successfully expressed in the ER (Fig. 3A). When these WFS1 mutant proteins were subjected to SDS/PAGE, HA-mWFS1(N663D/N748D) migrated faster than the HA-wild-type mWFS1 protein, while both HA-mWFS1(N663D) and HA-mWFS1(N748D) mutants were between the two (Fig. 3B). These results suggested that both asparagine residues, 663 and 748, are glycosylation sites and place the C-terminal stretch of WFS1 protein within the intraluminal compartment. Furthermore, as shown in Fig. 3C, although endoglycosidase H (Endo H) treatment of the wild-type WFS1 protein resulted in faster migration of the protein, the mobility of the double mutant [WFS1 (N663D/N748D)] protein was not affected by treatment with Endo H. In addition, the double mutant protein exhibited the same mobility as the wild-type WFS1 protein treated with Endo H. These data demonstrated that no asparagine residue other than N663 and N748 is glycosylated.

Reduced protein stability of N-glycosylation-defective WFS1 protein

N-glycosylation reportedly plays an important role in the stability of proteins such as the T cell antigen receptor α-subunit [16], the α-subunit of the nicotinic acetylcholine receptor [17], and apolipoprotein B [18]. Therefore, to assess the role of N-glycosylation in WFS1 protein stability, we performed pulse-chase

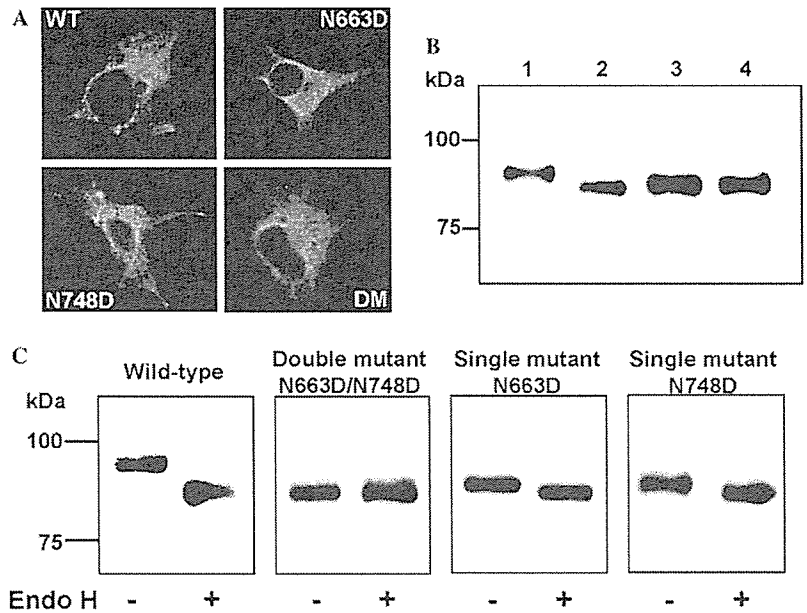

Fig. 3. Electrophoretic mobility and effect of endoglycosidase digestion on HA-tagged wild-type and mutant WFS1 proteins. (A) Immunofluorescence localization of HA-tagged WFS1 proteins: upper left, wild-type HA-mWFS1; upper right, HA-mWFS1(N663D); lower left, HA-mWFS1(N748D); lower right, HA-mWFS1(N663D/N748D). (B) COS7 cells transfected with 0.5 μg plasmids encoding either HA-tagged wild-type or mutant WFS1 proteins were lysed, subjected to SDS/PAGE, and probed with anti-HA antibody: lane 1, HA-mWFS1; lane 2, HA-mWFS1 (N663D/N748D); lane 3, HA-mWFS1(N663D); and lane 4, HA-mWFS1(N748D). (C) Lysates of COS7 cells transfected with either wild-type WFS1 cDNA or mutant constructs were incubated at 37 °C for 1 h with or without endoglycosidase H (500 U) and were subjected to electrophoresis on NuPAGE 3–8% Tris–acetate gel.

experiments. In these experiments, COS7 cells transiently transfected with either the HA-wild-type mWFS1 or mutant HA-mWFS1(N663D/N748D) cDNAs were labeled for 3 h with [^{35}S]methionine/cysteine and chased for different intervals. As shown in Fig. 4, the wild-type mWFS1 protein was relatively stable; 65 ± 6% ($n = 3$) of the protein remained 18 h after its synthesis. In contrast, only 44 ± 5% ($n = 3$) of mWFS1(N663D/N748D) remained after 18 h. These data showed protein stability to be reduced when both N-glycosylation sites were disrupted. One could argue an increased turnover rate of mWFS1(N663D/N748D) to be due to introducing aspartate residues rather than lack of glycosylation. To study the roles of N-glycosylation in various glycoproteins, asparagine residues in the consensus motif have been substituted with a variety of amino acids, such as aspartate ([19,20], this study), glutamine [14,21], alanine [19,22], threonine [23], and isoleucine [24]. None of these replacements were perfect, because introducing different residues might have its own effects. In this study, we also observed that WFS1 protein in MIN6 cells was more rapidly degraded when treated with a glycosylation inhibitor, tunicamycin (Fig. 1E). Thus, both molecular and biochemical approaches indicated that glycosylation-defective WFS1 protein has reduced stability. We therefore conclude that N-glycosylation affects WFS1 protein levels. A previous study using the ER resident glycoprotein ribophorin showed N-glycosylation to be necessary for calnexin binding, which prevents the glycoprotein from being rapidly degraded [25]. Such a mechanism could also be operative in WFS1 protein.

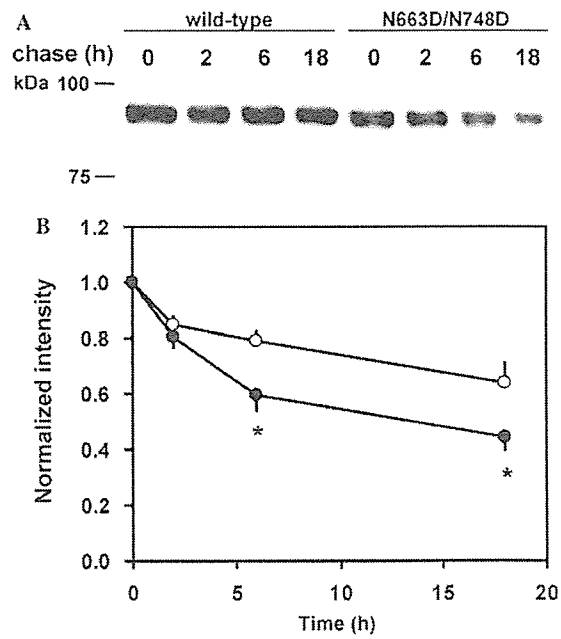

Fig. 4. Decreased stability of glycosylation-defective WFS1 protein. (A) HA-mWFS1 and HA-mWFS1(N663D/N748D) profiles of radiolabeled bands as a function of time of chase. A representative result from three experiments is shown. (B) Data from three experiments are summarized after normalization to time zero of chase. *$P < 0.05$.

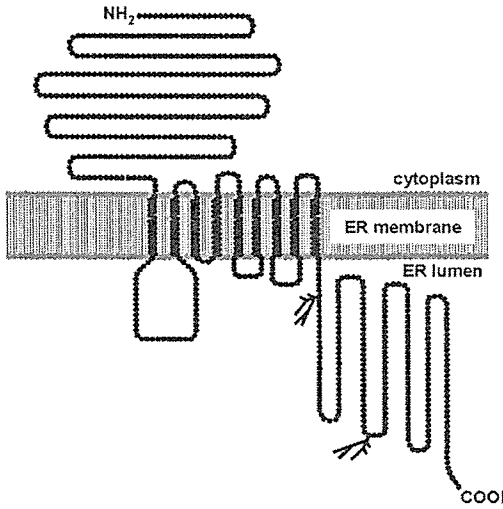

Fig. 5. Transmembrane topology model for mouse WFS1 protein with glycosylation sites. Membrane topology of mouse WFS1 protein as based on analysis using the SOSUI computer program [26] and data obtained in this study. Two N-glycosylation sites in the C-terminus stretch are depicted.

Herein, we defined the membrane topology of WFS1 by analyzing protease protection susceptibility: the orientation of the N-terminus in the cytoplasm and the C-terminus in the ER. This topology was supported by determining the N-glycosylation sites to be N663 and N748. A schematic diagram of WFS1 protein deduced from the current study and others is shown in Fig. 5. WFS1 protein/wolframin is a type II transmembrane protein and has long N-terminal and C-terminal stretches. These stretches could interact with other molecule(s), thereby mediating specific functions. Further study of these actions is clearly warranted. N663 and N748 residues in murine WFS1 protein correspond to N661 and N746 in the human orthologue. Although more than 100 mutations have been identified in WFS1 protein/wolframin and span the entire coding sequence, no mutations in these asparagine residues or adjacent amino acids were found in patients with Wolfram syndrome or LFSNHL. Given that loss of the functions of this protein is at least one of the pathogenic mechanisms of Wolfram syndrome [6,15], future survey of genomic sequences in patients with these diseases might identify mutations in these glycosylation sites.

The present data also provide evidence that increased WFS1 expression is the primary response of this protein to ER stress. There is no increase in WFS1 protein expression in response to tunicamycin, despite increased WFS1 mRNA levels. This is apparently attributable to the combined effects of increased mRNA levels and reduced protein stability. The increased WFS1 expression in response to ER-stress raises the possibility that WFS1 protein is a component of the UPR and plays a protective role against ER stress. This notion is supported by our recent findings that islets isolated from WFS1-deficient mice exhibited increased susceptibility to ER stress-induced apoptosis [7].

Acknowledgments

We are grateful to Y. Nagura for her expert technical assistance. This work was supported by a grant from Suzuken Memorial Foundation to H.I. and a Grant-in-Aid for Scientific Research (13204062) to Y.O. from the Ministry of Education, Science, Sports and Culture of Japan.

References

[1] K. Takeda, H. Inoue, Y. Tanizawa, Y. Matsuzaki, J. Oba, Y. Watanabe, K. Shinoda, Y. Oka, WFS1 (Wolfram syndrome 1) gene product: predominant subcellular localization to endoplasmic reticulum in cultured cells and neuronal expression in rat brain, Hum. Mol. Genet. 10 (2001) 477–484.

[2] H. Inoue, Y. Tanizawa, J. Wasson, P. Behn, K. Kalidas, E. Bernal-Mizrachi, M. Mueckler, H. Marshall, H. Donis-Keller, P. Crock, D. Rogers, M. Mikuni, H. Kimashiro, K. Higashi, G. Sobue, Y. Oka, M.A. Permutt, A gene encoding a transmembrane protein is mutated in patients with diabetes mellitus and optic atrophy (Wolfram syndrome), Nat. Genet. 20 (1998) 143–148.

[3] T.M. Strom, K. Hoetnagael, S. Hofmann, F. Gekeler, C. Scharfe, W. Rabl, K.D. Gerbitz, T. Meitinger, Diabetes insipidus, diabetes mellitus, optic atrophy and deafness (DIDMOAD) caused by mutations in a novel gene (wolframin) coding for a predicted transmembrane protein, Hum. Mol. Genet. 7 (1998) 2021–2028.

[4] I.N. Bespalova, G. Van Camp, S.J. Bom, D.J. Brown, K. Cryns, A.T. DeWan, A.E. Erson, K. Flothmann, H.P. Kunst, P. Kurnool, T.A. Sivakumaran, W.W.R.J. Cremers, S.M. Leal, M. Burmeister, M.M. Lesperance, Mutations in the Wolfram syndrome 1 gene (*WFS1*) are a common cause of low frequency sensorineural hearing loss, Hum. Mol. Genet. 15 (2001) 2501–2508.

[5] T.L. Young, E. Ives, E. Lynch, R. Person, S. Snook, L. MacLaren, T. Cater, A. Griffin, B. Fernandez, M.K. Lee, M.-C. King, Non-syndromic progressive hearing loss DFNA38 is caused by heterozygous missense mutation in the Wolfram syndrome gene WFS1, Hum. Mol. Genet. 15 (2001) 2509–2514.

[6] K. Cryns, T.A. Sivakumaran, J.M. Van den Ouweland, R.J. Pennings, C.W. Cremers, K. Flothmann, T.L. Young, R.J. Smith, M.M. Lesperance, G. Van Camp, Mutational spectrum of the WFS1 gene in Wolfram syndrome, nonsyndromic hearing impairment, diabetes mellitus, and psychiatric disease, Hum. Mutat. 22 (2003) 275–287.

[7] H. Ishihara, S. Takeda, A. Tamura, R. Takahashi, S. Yamaguchi, D. Takei, T. Yamada, H. Inoue, H. Soga, H. Katagiri, Y. Tanizawa, Y. Oka, Disruption of the WFS1 gene in mice causes progressive beta-cell loss and impaired stimulus-secretion coupling in insulin secretion, Hum. Mol. Genet. 13 (2004) 1159–1170.

[8] R. Kaufmann, Orchestrating the unfolded protein response in health and disease, J. Clin. Invest. 110 (2002) 1389–1398.

[9] H.P. Harding, D. Ron, Endoplasmic reticulum stress and the development of diabetes, Diabetes 51 (Suppl. 3) (2002) S455–S461.

[10] A.A. Osman, M. Saito, C. Makepeace, M.A. Permutt, P. Schlesinger, M. Mueckler, Wolframin expression induces novel ion channel activity in endoplasmic reticulum membranes and increases intracellular calcium, J. Biol. Chem. 278 (2003) 52755–52762.

[11] K. Cryns, S. Thys, L. van Laer, Y. Oka, M. Pfister, L. van Nassauw, R.J.H. Smith, J.P. Timmermans, G. Van Camp, The WFS1 gene, responsible for low frequent sensorineural hearing loss and Wolfram syndrome, is expressed in a variety of inner ear cells, Histochem. Cell Biol. 119 (2003) 247–256.
[12] H. Ishihara, T. Asano, K. Tsukuda, H. Katagiri, K. Inukai, M. Anai, M. Kikuchi, Y. Yazaki, J.I. Miyazaki, Y. Oka, Pancreatic beta cell line MIN6 exhibits characteristics of glucose metabolism and glucose-stimulated insulin secretion similar to those of normal islets, Diabetologia 36 (1993) 1139–1145.
[13] K.F. Ferri, G. Koemer, Organelle-specific initiation of cell death pathways, Nat. Cell Biol. 3 (2001) E255–E263.
[14] T. Michikawa, H. Hamanaka, H. Otsu, A. Yamamoto, A. Miyawaki, T. Furuichi, Y. Tashiro, K. Mikoshiba, Transmembrane topology and sites of N-glycosylation of inositol 1,4,5-trisphosphate receptor, J. Biol. Chem. 269 (1994) 9184–9189.
[15] S. Hofmann, C. Philbrook, K.D. Gerbitz, M.F. Bauer, Wolfram syndrome: structural and functional analyses of mutant and wild-type wolframin, the WFS1 gene product, Hum. Mol. Genet. 12 (2003) 2003–2012.
[16] K.P. Kearse, D.B. Williams, A. Singer, Persistence of glucose residues on core oligosaccharides prevents association of TCR alpha and TCR beta proteins with calnexin and results specifically in accelerated degradation of nascent TCR alpha proteins within the endoplasmic reticulum, EMBO J. 273 (1994) 17064–17072.
[17] S.H. Keller, J. Lindstrom, P. Taylor, Inhibition of glucose trimming with castanospermine reduces calnexin association and proteosome degradation of the alpha-subunit of the nicotinic acetylcholine receptor, J. Biol. Chem. 273 (1998) 17064–17072.
[18] Y. Chen, F. Caherec, S.L. Chuck, Calnexin and other factors that alter translocation affects the rapid binding of ubiquitin to apoB in the Sec61 complex, J. Biol. Chem. 273 (1998) 11887–11894.
[19] T.K. Lee, A.S. Koh, Z. Cui, R.H. Pierce, N. Ballatori, N-glycosylation controls functional activity of Oatp1, an organic anion transporter, Am. J. Physiol. Gastrointest. Liver Physiol. 285 (2003) G371–G381.
[20] L. Niu, M.L. Heaney, J.C. Vera, D.W. Golde, High-affinity binding to the GM-CSF receptor requires intact N-glycosylation sites in the extracellular domain of the β subunit, Blood 95 (2000) 3357–3362.
[21] Q. Gong, C.L. Anderson, C.T. January, Z. Zhou, Role of glycosylation in cell surface expression and stability of HERG potassium channels, Am. J. Physiol. Heart Circ. Physiol. 283 (2002) H77–H84.
[22] J. He, A.M. Castleberry, A.G. Lau, R.A. Hall, Glycosylation of β_1-adrenergic receptors regulates receptor surface expression and dimerization, Biochem. Biophys. Res. Commun. 297 (2002) 565–572.
[23] N. Buhlmamm, A. Aldecoa, K. Leuthauser, R. Gujer, R. Muff, J.A. Fischer, W. Born, Glycosylation of the calcitonin receptor-like receptor at Asn(60) or Asn(112) is important for cell surface expression, FEBS Lett. 486 (2000) 320–324.
[24] M. Ramanujam, J. Hofmann, H.L. Nakhasi, C.D. Atreya, Effect of site-directed asparagine to isoleucine substitutions at the N-linked E1 glycosylation sites on rubella virus viability, Virus Res. 81 (2001) 151–156.
[25] M. de Virgilio, C. Kitzmueller, E. Schwaiger, M. Klein, G. Kreibich, N.E. Ivessa, Degradation of a short-lived glycoprotein from the lumen of the endoplasmic reticulum: the role of N-inked glycans and the unfolded protein response, Mol. Biol. Cell 10 (1999) 4059–4073.
[26] T. Hirokawa, S. Boon-Chieng, S. Mitaku, SOSUI: classification and secondary structure prediction system for membrane proteins, Bioinformatics 14 (1998) 378–379.

Dissipating Excess Energy Stored in the Liver Is a Potential Treatment Strategy for Diabetes Associated With Obesity

Yasushi Ishigaki,[1] Hideki Katagiri,[2] Tetsuya Yamada,[1] Takehide Ogihara,[2] Junta Imai,[1,2] Kenji Uno,[1,2] Yutaka Hasegawa,[1,2] Junhong Gao,[1,2] Hisamitsu Ishihara,[1] Tooru Shimosegawa,[3] Hideyuki Sakoda,[4] Tomoichiro Asano,[4] and Yoshitomo Oka[1]

For examining whether dissipating excess energy in the liver is a possible therapeutic approach to high-fat diet–induced metabolic disorders, uncoupling protein-1 (UCP1) was expressed in murine liver using adenoviral vectors in mice with high-fat diet–induced diabetes and obesity, and in standard diet–fed lean mice. Once diabetes with obesity developed, hepatic UCP1 expression increased energy expenditure, decreased body weight, and reduced fat in the liver and adipose tissues, resulting in markedly improved insulin resistance and, thus, diabetes and dyslipidemia. Decreased expressions of enzymes for lipid synthesis and glucose production and activation of AMP-activated kinase in the liver seem to contribute to these improvements. Hepatic UCP1 expression also reversed high-fat diet–induced hyperphagia and hypothalamic leptin resistance, as well as insulin resistance in muscle. In contrast, intriguingly, in standard diet–fed lean mice, hepatic UCP1 expression did not significantly affect energy expenditure or hepatic ATP contents. Furthermore, no alterations in blood glucose levels, body weight, or adiposity were observed. These findings suggest that ectopic UCP1 in the liver dissipates surplus energy without affecting required energy and exerts minimal metabolic effects in lean mice. Thus, enhanced UCP expression in the liver is a new potential therapeutic target for the metabolic syndrome. ***Diabetes*** **54:322–332, 2005**

From the [1]Division of Molecular Metabolism and Diabetes, Tohoku University Graduate School of Medicine, Sendai, Japan; the [2]Division of Advanced Therapeutics for Metabolic Diseases, Center for Translational and Advanced Animal Research, Tohoku University Graduate School of Medicine, Sendai, Japan; the [3]Division of Gastroenterology, Tohoku University Graduate School of Medicine, Sendai, Japan; and the [4]Department of Internal Medicine, Faculty of Medicine, University of Tokyo, Tokyo, Japan.

Address correspondence and reprint requests to Hideki Katagiri, MD, PhD, Division of Advanced Therapeutics for Metabolic Diseases, Center for Translational and Advanced Animal Research, Tohoku University Graduate School of Medicine, 2-1 Seiryo-machi, Aoba-ku, Sendai 980-8575, Japan. E-mail: katagiri-tky@umin.ac.jp.

Received for publication 19 April 2004 and accepted in revised form 13 October 2004.

Y.I., H.K., and T.Y. contributed equally to this work.

ACC1, acetyl-CoA carboxylase 1; AMPK, AMP-activated protein kinase; CPT1, carnitine palmitoyltransferase 1; IRS1, insulin receptor substrate 1; PPAR, peroxisome proliferator–activated receptor; SREBP, sterol regulatory element binding protein; TNF-α, tumor necrosis factor-α; UCP, uncoupling protein.

An explosive increase in the number of diabetic patients, which has become a major public health concern in most industrialized countries in recent decades (1), is mainly the result of excess energy intake and physical inactivity. When food intake chronically exceeds metabolic needs, efficient metabolism causes excess energy storage and results in obesity, a common condition associated with diabetes, hyperlipidemia, and premature heart disease. Excess energy in cells lowers the response to insulin, namely insulin resistance. However, the major treatment modalities for diabetes, including insulin injection and oral sulfonylureas, aim at lowering blood glucose levels by driving glucose into cells in peripheral tissues such as muscle and fat. This further exacerbates insulin resistance when energy intake is in excess, resulting in a vicious cycle. Therefore, novel therapies that promote increased energy expenditure are needed.

Inefficient metabolism, such as the generation of heat instead of ATP, is a potential treatment strategy for type 2 diabetes associated with obesity. Uncoupling proteins (UCPs) were discovered members of the mitochondrial inner membrane carrier family. These proteins leak protons into the mitochondrial matrix, dissipating energy as heat rather than allowing it to be captured in ATP (2). UCP1 (thermogenin) was originally identified in brown adipose tissue and demonstrated to mediate nonshivering thermogenesis. UCP1 plays an important role in mediating cold exposure–induced thermogenesis (3) and is also a likely regulator of diet-induced thermogenesis (4).

Several laboratories have reported overexpression of UCPs, using the transgenic approach, in mice (5–8). These reports indicate that overexpression of UCPs in white adipose tissue and skeletal muscle has preventive effects on development of genetic and dietary obesity and the resultant insulin resistance. However, it is still unclear whether ectopic UCP1 expression exerts therapeutic effects after the development of diabetes associated with obesity.

The liver is one of the major metabolic organs involved in glucose and lipid metabolism and insulin action. In addition, the liver can store and release abundant fat